Full System Modeling and Validation of the Carbon Dioxide Removal Assembly

Robert Coker, James Knox, Hernando Gauto, Carlos Gomez
MSFC, NASA, Huntsville, AL 35812

The Atmosphere Revitalization Recovery and Environmental Monitoring (ARREM) project was initiated in September of 2011 as part of the Advanced Exploration Systems (AES) program. Under the ARREM project, testing of sub-scale and full-scale systems has been combined with multiphysics computer simulations for evaluation and optimization of subsystem approaches. In particular, this paper describes the testing and modeling of various subsystems of the carbon dioxide removal assembly (CDRA). The goal is a full system predictive model of CDRA to guide system optimization and development. The development of the CO_2 removal and associated air-drying subsystem hardware under the ARREM project is discussed in a companion paper.

Nomenclature

a_0	=	constant in single-species Toth equation, mol kg^{-1} kPa^{-1}
E	=	constant in single-species Toth equation, K
c_0	=	constant in single-species Toth equation, K
b_0	=	constant in single-species Toth equation, kPa^{-1}
t_0	=	constant in single-species Toth equation
a	=	single-species Toth equation parameter, mol kg^{-1} kPa^{-1}
b	=	single-species Toth equation parameter, kPa^{-1}
t_T	=	single-species Toth equation parameter
B	=	length of test bed filled with sorbent, m
R_B	=	radius of sorbet-filled test bed cylinder, m
d	=	thickness of test bed cylinder, m
$\varepsilon_{sorbent}$	=	porosity in the sorbent bed
ρ	=	density, kg m^{-3}
$D_{pellets}$	=	mean diameter of sorbent pellets, m
$\kappa_{sorbent}$	=	permeability through the sorbent beds, m^2
κ_f	=	permeability correction factor
u	=	velocity, m s^{-1}
u_{in}	=	flow velocity at inlet, m s^{-1}
P	=	pressure, Pa
R_s	=	specific gas constant, J kg^{-1} K^{-1}
R_g	=	universal gas constant, J mol^{-1} K^{-1}
M_{mix}	=	molecular mass of gas mixture, kg mol^{-1}
Mu	=	viscosity, Pa-s
T	=	temperature, K
$T_{gin}(t)$	=	measured time-dependent inlet temperature of gas, K
$P_{vapin}(t)$	=	measured time-dependent inlet sorbate partial pressure, Pa
P_{vap}	=	sorbate partial pressure, Pa
P_{out}	=	calculated absolute pressure at bed exit, Pa
P_{in}	=	measured absolute pressure at bed inlet, Pa
ΔP	=	measured pressure drop across bed, Pa
F	=	flowrate, SLPM
A	=	ratio of total sorbent surface area to sorbent volume, m^{-1}
A_f	=	free flow area of can inlet, m^2
A_c	=	cross sectional area of the can, m^2

P_0 = reference pressure, Pa
T_0 = reference temperature, K
P_O = outer perimeter of test can, m
P_I = inner perimeter of test can, m
c = concentration of sorbate, mol m^{-3}
q = pellet loading, mol m^{-3}
q_* = equilibrium pellet loading, mol m^{-3}
c_{in} = concentration of sorbate at inlet, mol m^{-3}
D_x = axial dispersion coefficient, m^2 s^{-1}
x = spatial coordinate, m
t = temporal coordinate, s
k_m = mass transfer coefficient, s^{-1}
c_p = heat capacity, J kg^{-1} K^{-1}
k = thermal conductivity, W m^{-1} K^{-1}
h = heat transfer coefficient, W m^{-2} K^{-1}
∂H = differential heat of adsorption, kJ mol^{-1}
f = directionally dependent coefficient for *Pe*
D_{AB} = binary mass diffusion coefficient, m^2 s^{-1}
Sc = Schmidt number
Re = Reynolds number
Pe = Peclet number
Nu = Nusselt number
Pr = Prandtl number
ARREM = Atmosphere Revitalization Recovery and Environmental Monitoring
AES = Advanced Exploration Systems
SG = Silica Gel
LPM = liters per minute
SLPM = standard (1 atm, 0 ºC) liters per minute
RHS = right hand side
CBT = cylindrical breakthrough test

Subscripts:
x = component in the x (axial) direction
r = component in the r (radial) direction
s = pertaining to the sorbent
g = pertaining to the gas
A = pertaining to the ambient environment
c = pertaining to the can housing

I. Introduction

PREDICTIVE simulation tools are being developed to reduce the hardware testing requirements of the Atmosphere Revitalization Recovery and Environmental Monitoring (ARREM) project as part of NASA's Advanced Exploration Systems (AES) program[1,2]. Although sub-scale testing is required to establish the predictive capability of the simulations, the much greater cost of extensive full-scale testing can be limited to that required for the confirmation of analytical design optimization studies. Once predicative capability is established, geometric reconfiguration of a model is usually straightforward. A predictive simulation capability provides improved understanding of complex processes since process conditions (temperature, pressure, concentrations, etc.) may be examined anywhere in the sorption column. Weaknesses in a prototype design can be readily identified and improvements tested via simulation. Finally, the predictive simulation provides a powerful tool for virtual troubleshooting of deployed flight hardware. Here, we discuss using the COMSOL Multiphysics code[3] to model in detail – and predictively – experiments that are similar to the desiccant subcomponent of a full Carbon Dioxide Removal Assembly (CDRA) system.

II. Design Approach Using COMSOL

Adsorption in packed fixed beds of pelletized sorbents is presently the primary means of gas separation for atmosphere revitalization systems. However, structured sorbents are emerging as a new approach to sorbent systems. Structured sorbents are produced as monoliths, with an open structure for airflow, or by fixing sorbents on an inert substrate such as paper-like honeycomb structures or expanded metal sheets. A well designed structured sorbent is not as subject to attrition (e.g., due to fines or dust generation) as a packed bed. Also, by using a thermally conductive substrate, the heat of adsorption can be transferred out of the bed, possibly to the cold desorbing bed if geometry permits. However, structured sorbents must be evaluated to determine their applicability to commercial processes and space flight. It must be shown that, in addition to providing a more robust solution, the resource requirements (i.e., weight, power, volume, etc.) are similar to, if not less than, the state-of-the-art packed bed configuration.

Figure 1. CBT Test Bed.

An accurate assessment of structured sorbents and comparison with packed bed designs is desirable; experimental results so far show unanticipated variation in packed bed breakthrough for identical beds held under the same conditions. It is suspected that small packing irregularities can propagate downstream in large beds and impact process efficiency. This indicates a margin of error inherent in packed bed fabrication and thus a likely superiority of structured sorbents for process efficiency and control. This paper discusses fully predictive modeling results using COMSOL's Multiphysics code for a geometrically simple fixed bed design. Insights learned from this work will be used in future modeling of the entire CDRA system.

For the bulk separation of CO_2 and H_2O, temperature changes due to the heat of adsorption are significant, requiring the simulation of the heat balance equations through the beds and the housing, as well as the equations for sorption processes and fluid flow. For columns with small tube diameter to pellet diameter ratios, as encountered in internally heated columns, flow channeling along the column wall can have a strong influence on overall performance. In non-cylindrical flow, the influence is great enough to necessitate the use of 3-D simulations. Here, with over a dozen pellets per cylinder diameter, 1-D models should prove accurate enough for predictively driven system design.

III. Cylindrical Breakthrough Test

A. Description

The CDRA requires a water-saving bulk drying stage prior to downstream CO_2 removal. The primary goal is to continuously remove at least 80% and up to 100% of water vapor from a process air stream. The Cylindrical Breakthrough Test (CBT) was constructed to compare sorption kinetics for various sorbent and sorbate pairs. The tests consist of flowing a constant amount of sorbate and carrier gas through a fixed bed containing a regenerated (or dried out) sorbent. After some period of time (the 'breakthrough time'), the sorbate is detected at the bed exit. A plot of the sorbate concentration or partial pressure versus time is the breakthrough curve. Axially routed thermocouples are used to acquire temperature curves inside and outside of the bed as well as before and after the

packed bed. The three thermocouples inside the bed are on axis and are located 1 inch inside the inlet and exit and in the axial middle of the sorbent-filled bed. Absolute and differential pressure is measured at the column inlet and across the column, respectively.

The test apparatus, shown in Fig. 1, was designed to have relatively low mass (to reduce regeneration time) and good axial symmetry (to reduce system complexity). The test bed, packed with regenerated sorbent pellets, is insulated to minimize system heat loss. Mass flow controllers are used to blend N_2, the carrier gas, with the desired partial pressure of CO_2 or H_2O. For CO_2 tests, Sable Systems CO_2 analyzers provide inlet and outlet CO_2 partial pressure readings, while for H_2O tests, a Sable Systems Dew Point Generator provides humidity control and Edgetech Dewmaster dew point analyzers provide inlet and outlet dew point measurements.

A schematic of the entire test setup is shown in Fig. 2. The cylindrical column of sorbent has a bed length, *B*, of 6.5 inches and a radius, R_B, of 1.74 cm. The mass of regenerated sorbent in the test bed is measured so as to determine the mean porosity of the bed. The Al 6061 housing is d=0.065 inches thick and extends for 6 inches upstream and downstream of the sorbent. The sorbent is held in place inside the housing using spring-loaded plates and fine mesh screens. Here, we focus on the CBT adsorption tests, where the sorbent starts fully regenerated. Experimental data from the CBT will be used to validate the simulation process so that simulation-driven optimization may be used alongside conventional design methods to perfect CDRA sub-component design and testing.

B. Models

1-D models of the CBT were constructed using the COMSOL Multiphysics code using Domain ODEs and DAEs. Only the sorbent-containing part of the bed is modeled. A constant porosity, $\epsilon_{sorbent}$, was used, such that, together with the known constant density of the sorbent, ρ_s, the proper measured total sorbent mass is recovered. Using the measured mean particle diameter of the sorbent pellets, $D_{pellets}$, the local permeability within each cell is then found[4]:

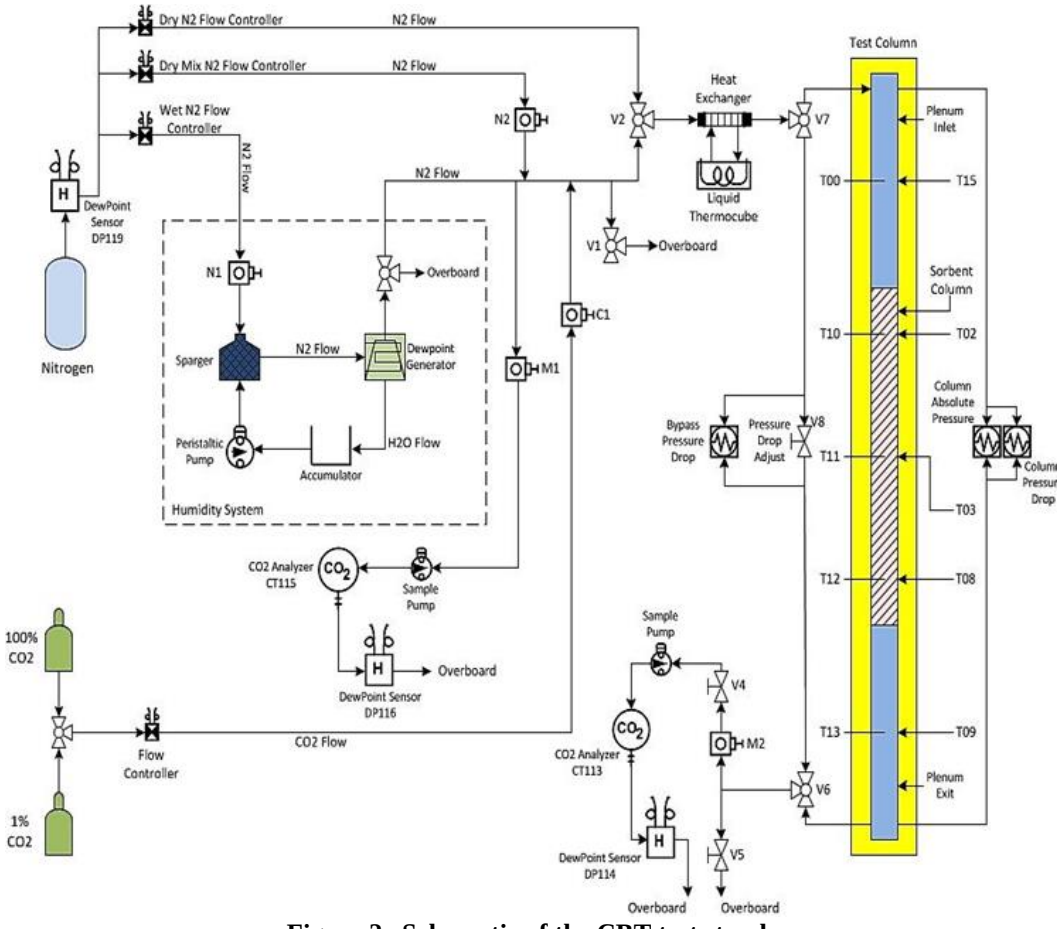

Figure 2. Schematic of the CBT test stand.

$$\kappa_{sorbent} = \frac{\kappa_f \, \epsilon_{sorbent}^{5.5} * D_{pellets}^{2}}{5.6} \quad (1).$$

However, the correct diameter to use in Eq.(1) is a volume-weighted averaged such as the Sauter mean, but this is not as well known as $D_{pellets}$ for all sorbents, but it is generally larger than $D_{pellets}$. The factor, κ_f, is adjusted to reproduce the measured pressure drop through the test bed for a given test (so it is not a free parameter). Since Eq.(1) was developed for typical sandstone packing, some sorbents that are very spherical and smooth have rather large values of κ_f. Note that for the CBT, the measured pressure drop is close to the analytical pressure drop predicted by the Ergun equation. Flow PDEs are derived based on simplification of the Navier-Stokes and Brinkman equations while assuming compressible flow; these are combined with PDEs for the loading, based on the Toth equations, the sorbate concentration, and the temperature of the gas mixture, sorbent pellets, and housing walls.

The first PDE finds the 1-D interstitial velocity, u:

$$\frac{P}{R_s T_g}\frac{\partial u}{\partial t} = -\left(\frac{\partial P}{\partial x} + \frac{u\mu}{\kappa_{sorbent}}\right) - \frac{u}{R_s}\frac{\partial\left(\frac{P}{T_g}\right)}{\partial t} \quad (2),$$

where P is the gas pressure, R_s is the mixture's specific gas constant (=R_g/M_{mix}), μ is the gas viscosity, and T_g is the temperature of the flowing gas mixture. Eq.(2) is essentially a 1st order Ergun[5] equation that reduces to Darcy's Law in steady state. The 2nd order Ergun term, somewhat akin to a Forchheimer drag term proportional to the square of the fluid velocity, was initially added to the RHS of Eq.(2), but the impact was negligible and so removed for the work discussed here. Here, for simplicity the molecular mass of the mixture, M_{mix}, is assumed to be that of the pure carrier gas, N_2. Note that the velocity, which is in the axial direction, is not compensated for loss of sorbate since the sorbate gas mole fraction is <<1. In COMSOL, the entirety of the RHS of Eq.(2) is written as a source term in the General Form PDE; the pressure gradient cannot be written as a conservative flux term or the boundary conditions become over-constrained. Also, Eq.(2) assumes the ideal gas law for the density of the gas mixture, so that:

$$\rho_g = \frac{P}{R_s T_g} \quad (3),$$

The second PDE solves for the gas pressure, P, using the continuity equation and Eq.(3):

$$\frac{\epsilon_{sorbent}}{R_s T_g}\frac{\partial P}{\partial t} + \frac{\partial}{\partial x}\left(\frac{uP}{R_s T_g}\right) - \frac{\epsilon_{sorbent}}{R_s T_g^{\,2}} P \frac{\partial T_g}{\partial t} = 0 \quad (4).$$

In COMSOL, in the Coefficient Form PDE, the 1st term of Eq.(4) is a Mass Coefficient term, the 2nd is a Convection term, and the 3rd is an Absorption Coefficient term. The outlet pressure boundary condition is of the Dirichlet type, using the measured outlet pressure from a given test, $P_{out} = P_{in} - \Delta P$. The inlet uses a mass flux boundary condition based on the measured constant standard flow rate, F, for a given test:

$$f_M = \frac{P_0}{R_s T_0}\,\frac{\mathrm{F}}{\epsilon_{sorbent} A_f} \quad (5),$$

where $A_f = \pi R_B^{\,2}$ is the inlet free flow area and P_0 and T_0 are the reference pressure and temperature, respectively, at which the flowrate is defined. Thus, the 1st term in Eq.(5) is a reference density. Here, P_0=1 atm and T_0=0°C. Since this is a 1-D 'plug flow' model, there is no gradient of pressure, velocity, concentration, temperature, or porosity in the radial direction.

The third and fourth PDEs are coupled and solve for sorbate concentration, c, and pellet loading, q, respectively. The latter applies the Linear Driving Force model[6]. Together these two PDEs are referred to as the 'Mass Balance' equations. The General Form PDEs are:

$$\frac{\partial c}{\partial t} + \frac{(1-\epsilon_{sorbent})}{\epsilon_{sorbent}}\frac{\partial q}{\partial t} + \frac{\partial}{\partial x}\left(-D_x \frac{\partial c}{\partial x}\right) = -\frac{\partial}{\partial x}(uc) \quad (6)$$

$$\frac{\partial q}{\partial t} = k_m(q_* - q) \quad (7),$$

where D_x is the local time-dependent axial mass dispersion coefficient, q_* is the equilibrium loading from the Toth isotherms, and k_m is the constant mass transfer coefficient (see below). For the concentration, a zero gradient Constraint:

$$\left.\frac{\partial c}{\partial x}\right|_{x=B} = 0 \quad (8),$$

is used at the exit, while a molar volume flux boundary condition is used at the inlet:

$$D_x \left.\frac{\partial c}{\partial x}\right|_{x=0} = (u_{in}c_{in} - uc) \quad (9),$$

where u_{in} = $f_M R_s T_{gin}(t)/P_{vapin}(t)$, is the inlet interstitial velocity and c_{in} = $P_{vapin}(t)/R_g/T_{gin}(t)$, is the sorbate concentration at the upstream inlet to the bed. $P_{vapin}(t)$ and $T_{gin}(t)$ are the measured time-dependent sorbate partial pressure and gas temperature, respectively, for each experiment. Since $T_{gin}(t)$ is measured far upstream of the start of the sorbent in the bed, the COMSOL inlet value is the measured value minus an offset of 1.2°C*8SLPM/F due to losses along the uninsulated piping. That is, this ensures that $T_{gin}(t=0)$ actually equals the $T(t=0,x=0)$ inside the bed for any given experiment. There are no explicit spatial boundary conditions required for Eq.(7) since there is no loading outside of the sorbent bed. In COMSOL, it is necessary to make the RHS of Eq.(6) a source term, rather than a flux term, in order to apply the inlet flux boundary condition properly. The above transport PDE, Eq.(6), represents Fickian diffusion[6] in conservative form and assumes that all mechanical dispersion effects are lumped together with molecular diffusion in the axial dispersion term.

The fifth, sixth, and seventh PDEs are coupled and solve for the sorbent temperature, T_s, the gas temperature, T_g, and the wall housing temperature, T_c, respectively. Together these are referred to as the 'Thermal Balance' equations. The General Form PDEs are:

$$(1-\epsilon_{sorbent})\rho_s c_{ps}\frac{\partial T_s}{\partial t} + \frac{\partial}{\partial x}\left(-k_s(1-\epsilon_{sorbent})\frac{\partial T_s}{\partial x}\right) = \mathrm{A}h_{sg}\left(T_g - T_s\right) - \partial\mathrm{H}(1-\epsilon_{sorbent})\frac{\partial q}{\partial t} \quad (10)$$

$$\epsilon_{sorbent}\rho_g c_{pg}\frac{\partial T_g}{\partial t} + \frac{\partial}{\partial x}\left(-k_{gx}\epsilon_{sorbent}\frac{\partial T_g}{\partial x}\right) = \mathrm{A}h_{sg}\left(T_s - T_g\right) - \epsilon_{sorbent}\rho_g c_{pg}u\frac{\partial T_g}{\partial x} + \frac{P_I h_{gc}\left(T_c - T_g\right)}{A_f} \quad (11)$$

$$\rho_c c_{pc}\frac{\partial T_c}{\partial t} + \frac{\partial}{\partial x}\left(-k_c\frac{\partial T_c}{\partial x}\right) = \frac{P_I h_{gc}\left(T_g - T_c\right)}{A_c} + \frac{P_O h_{Ac}(T_A - T_c)}{A_c} \quad (12).$$

Again, all of the terms on the RHS of Eqs.(10-12) are source terms in COMSOL. Since u_s and u_w are identically zero everywhere (thus, $u \equiv u_g$ explicitly throughout this document), no explicit boundary conditions are required for Eqs.(10 and 12). In Eqs.(10-12), subscripts *s*, *g*, *A*, and *c* refer to properties of the sorbent, gas mixture, ambient environment, and can housing, respectively. $P_I = 2\pi R_B$, $P_O = 2\pi(R_B+d)$, and $A_c = \pi((R_B+d)^2 - R_B^2)$ are the can inner perimeter, outer perimeter, and cross sectional area, respectively. Heat capacity, thermal conductivity, and thermal transfer coefficients are given by c_p, *k*, and *h*, respectively. The heat of adsorption for a given sorbate/sorbent pair is given by ∂H and is assumed constant (see Table 1 below). The ratio of sorbent area to volume assumes spherical pellets and is given by $A = (1-\epsilon_{sorbent})6A_f/D_{pellets}$. The outlet boundary condition for Eq.(11) is given by a zero gradient Constraint:

$$\left.\frac{\partial T_g}{\partial x}\right|_{x=B} = 0 \ (13),$$

while the inlet is given by a flux boundary condition:

$$k_{gx}\left.\frac{\partial T_g}{\partial x}\right|_{x=0} = \rho_g c_{pg} u\left(T_{gin}(t) - T_g\right) \quad (14).$$

The initial conditions for the *c* and *q* PDEs correspond to equilibrium loading for a small initial sorbate partial pressure, typically 1-5 Pa. The initial velocity is u_{in} everywhere, while the initial pressure is set to P_{in}-ΔP*x/*B*. All temperatures are initially uniform and set to the measured (but offset) $T_{gin}(t = 0)$.

The boundary conditions described above for *P*, *T*, and *c* are all the measured values from a given test, with *T* and *c* being time-dependent. This is necessary since, as will be seen below, the variation from test to test (or even within a single test), even using the same packed bed and nominal test conditions for flow rate and inlet sorbate partial pressure, is often larger than the uncertainty in the model.

1. *Dimensionless Numbers*

Many of the physical parameters used in Eqs.(10-12) are determined from correlations based on dimensionless quantities. The empirical relationships used here are appropriate for 1-D models in the regime of the CBT. The Schmidt number, *Sc*, pellet Reynolds number, *Re*, Peclet number[7], *Pe*, Prandtl number, *Pr*, gas to sorbent Nusselt number, Nu_{GS}[8], and gas to can Nusselt number, Nu_{GC}[9], are given by:

$$Sc = \frac{\mu}{\rho_g D_{AB}} \quad (15)$$

$$Re = \frac{u\rho_g D_{pellets}}{\mu} \quad (16)$$

$$Pe_{(x,r)} = \left(\frac{0.73\epsilon_{sorbent}}{ReSc} + \frac{1}{f_{(x,r)}\left(1 + \frac{13 * 0.73\epsilon_{sorbent}}{ReSc}\right)} \right)^{-1} \quad (17)$$

$$Pr = \frac{\mu c_{pg}}{k_g} \quad (18)$$

$$Nu_{GS} = 2 + 1.1\, Pr^{1/3} Re^{0.6} \quad (19)$$

$$Nu_{GC} = 2.63\, Re^{0.8} e^{-3D_{pellets}/R_B} \quad (20).$$

In Eq.(17), $f_{(x,r)}$ is 2 for axial (Pe_x) and 10 for radial (Pe_r) parameters. In Eq.(15), D_{AB} is the binary mass diffusion coefficient[10] for either water vapor or carbon dioxide in N_2 as a function of *P* and T_g.

2. *Toth*

The loading equation uses the Toth isotherm relationships:

$$q_* = \frac{aP_{vap}}{\left(1 + \left(bP_{vap}\right)^{t_T}\right)^{1/t_T}} \quad (21)$$

$$b = b_0 e^{E/T_g} \quad (22)$$

$$\mathrm{a} = a_0 e^{E/T_g} \quad (23)$$

$$t_T = t_0 + \frac{c_0}{T_g} \quad (24),$$

where $P_{vap} = c\ R_g\ T_g$ is the sorbate partial pressure and a_0, b_0, t_0, c_0, and *E* are Toth coefficients for a given sorbent/sorbate pair. The coefficients used[12] are listed in Table 1, together with the heat of adsorption[12,13] for each pair. It is known that ∂H depends on loading, decreasing significantly as equilibrium loading is approached; the quantitative dependence, however, is not well known for many sorbents, so the impact is left for future work. For the silica gel sorbents, Grace Grade 40 and Sylobead B125, the same Toth parameters are used, even though they are experimentally derived from the former. The same is true for the 5A zeolite sorbents, Grace Grade 522 and RK-38. There are no CBT experiments as yet with H_2O/5A or CO_2/SG systems.

Table 1. Adsorption Parameters for Sorbent/Sorbate Pairs

Sorbate/Sorbent System	a_0 mol kg^{-1} kPa^{-1}	b_0 kPa^{-1}	E K	t_0	c_0 K	∂H kJ mol^{-1}
CO_2/5A	9.875x10^{-7}	6.761x10^{-8}	5.625x10^{3}	2.700x10^{-1}	-2.002x10^{1}	-38.0
H_2O/5A	1.106x10^{-8}	4.714x10^{-10}	9.955x10^{3}	3.548x10^{-1}	-5.114x10^{1}	-45.0
CO_2/13X	6.509x10^{-3}	4.884x10^{-4}	2.991x10^{3}	7.487x10^{-2}	3.805x10^{1}	-40.0
H_2O/13X	3.634x10^{-6}	2.408x10^{-7}	6.852x10^{3}	3.974x10^{-1}	-4.199	-55.0
CO_2/SG	7.678x10^{-6}	5.164x10^{-7}	2.330x10^{3}	-3.053x10^{-1}	2.386x10^{2}	-40.0
H_2O/SG	1.767x10^{2}	2.787x10^{-5}	1.093x10^{3}	-1.190x10^{-3}	2.213x10^{1}	-50.2

3. *Material Properties*

Here the expressions for material properties are given. Some are from COMSOL's material libraries and some use the correlations in the previous section. Temperatures in the following expressions are in Kelvin and the derived values are in MKS units.

The axial mass dispersion coefficient used in Eq.(6) for the transport of the sorbate through the bed is given by:

$$D_x = \frac{uD_{pellets}}{Pe_x} (25).$$

For the gas mixture, COMSOL expressions for N_2 are used:

$$k_g = 3.6969697\text{x}10^{-4} + 9.74353924\text{x}10^{-5}T_g - 4.07587413\text{x}10^{-8}T_g^2 + 7.68453768\text{x}10^{-12}T_g^3 \quad (26)$$

$$k_{gx} = c_{pg}\rho_g D_x \quad (27)$$

$$c_{pg} = 1088.22121 - 0.365941919T_g + 7.88715035\text{x}10^{-4}T_g^2 - 3.749223\text{x}10^{-7}T_g^3 + 3.17599068\text{x}10^{-11}T_g^4 \quad (28)$$

$$\mu = 1.77230303\text{x}10^{-6} + 6.27427545\text{x}10^{-8}T_g - 3.47278555\text{x}10^{-11}T_g^2 + 1.01243201\text{x}10^{-14}T_g^3 \quad (29).$$

The effective axial gas thermal conductivity, k_{gx}, comes from a similarity assumption[6], which may not be valid in all regimes. The resulting values are typically as much as 50% larger than when using other, more complicated expressions[14].; the impact of different k_{gx} expressions on the breakthrough curves discussed here is minor.

For the can properties, COMSOL functions for Al 6061 are used:

$$k_c = 30.71577 + 0.8750948T_c - 0.002142331T_c^2 + 2.05104\text{x}10^{-6}T_c^3 \ , T_c < 300$$
$$= 79.478 + 0.3355001T_c - 2.701638\text{x}10^{-4}T_c^2, \quad T_c > 300 (30)$$

$$c_{pc} = -5.605966 + 6.744725T_c - 0.01535912T_c^2 + 1.619759\text{x}10^{-5}T_c^3 - 6.214813\text{x}10^{-9}T_c^4 \quad (31)$$

$$\rho_c = -2736.099 - 0.00940624T_c - 6.040342\text{x}10^{-4}T_c^2 + 8.988964\text{x}10^{-7}T_c^3 - 5.405225\text{x}10^{-10}T_c^4 \quad (32)$$

Note the piecewise expression used for k_c.

For the sorbent properties, since they are not well known, constant values are used[12,15,16]. They are listed for the sorbents used in this work in Table 2. For Sylobead B152, the sorbent density and heat capacity are assumed to be the same as for Grace Grade 40. Also listed in Table 2 are the mean pellet diameter, total dry sorbent mass, and resulting mean porosity for the sorbent packings used in the CBT experiments. The heat capacity of the pellets can change significantly as they get loaded. Thus, using, from COMSOL, the heat capacities of water vapor:

$$c_{pH2O} = 1.244444465\text{x}10^{-10}T_s^6 - 2.1702974711043\text{x}10^{-7}T_s^5 + 0.00015762822131718 1T_s^4 - 0.0610285680460429T_s^3 + 13.28450401510 98T_s^2 - 1541.53249062843T_s + 74503.5945678409 (33),$$

And of carbon dioxide:

$$c_{pCO2} = 459.913258 + 1.86487996T_s - 0.00212921519T_s^2 + 1.22488004\text{x}10^{-6}T_s^3 (34),$$

a mass-weighted loading-dependent effective heat capacity can then be used for c_{ps}:

$$c_{ps} = \frac{\left(c_{p(H2O,CO2)} qM_{(H2O,CO2)} + c_{ps0}\rho_s\right)}{\left(qM_{(H2O,CO2)} + \rho_s\right)} \quad (35).$$

Eq.(35) typically reduces the pellet heat capacity by ~10% when the sorbate is H_2O, but is insignificant for CO_2.

The thermal transfer coefficients for the gas are determined from *Nu*:

$$h_{sg} = Nu_{GS}\rho_g / D_{pellets} \quad (36)$$

$$h_{gc} = \frac{Nu_{GC}\rho_g}{(2R_B)} \quad (37),$$

while for the ambient to can heat transfer, a nominal constant small value of h_{Ac}=0.1 W/m^2/K was used, since the insulation was not firmly bonded with the cylinder. As a result, the value used for T_A, the ambient temperature, is not very critical, so a constant 19°C value, representative of the CBT laboratory, was used in this work. However, varying T_A to the measured value for each test (when available) would result in slightly improved late time temperature profiles (see below). Also, h_{sg} is typically ~150 W/m^2/K, so the gas and sorbent are well thermally coupled, while h_{gc} is typically ~25 W/m^2/K, so the can is less coupled to the flow. As a result, in the results discussed below, typically,$|T_g\text{-}T_s|$ <<1°C and $|T_g\text{-}T_c|$ >>1°C.

Table 2. Properties of Sorbents as Packed in the CBT

Sorbent	ρ_s kg m^{-3}	c_{ps0} (@26°C) J kg^{-1} K^{-1}	k_s W m^{-1} K^{-1}	$D_{pellets}$ mm	mass g	$\epsilon_{sorbent}$
5A (Grace Grade 522)	1190	750	0.152	2.22	125.0	0.331
5A (RK38)	1370	650	0.144	2.10	119.3	0.445
13X (Grace Grade 544)	1260	800	0.147	2.19	107.4	0.457
SG (Grace Grade 40)	1240	870	0.165	2.90	111.7	0.415
SG (Sylobead B125)	1240	870	0.151	2.25	127.0	0.348

C. COMSOL Results

The only free parameter required to fit the CBT data is k_m, the mass transfer coefficient used in the LDF model (see Eq.(7)). It is not expected to be sensitive to different test conditions, such as flow rates, vapor pressure, or temperatures. Ideally, it is only a function of the sorbent/sorbate pairing, but in practice it can vary due to, for example, geometry differences when R_B is only a few times $D_{pellets}$, making arbitrary predictive applications with the LDF model problematic. Here, the same value of k_m is used for all CBT experiments of a given sorbent/sorbate pairing. Note that k_m drives the slope of the vapor pressure rise curve, so for the model to be self-consistent, it should reproduce that slope; that is, even k_m is not a true free parameter even for a single test of a given sorbent/sorbate pairing. The intent is to derive k_m for a given sorbent/sorbate pair and use it in future predictive modeling of CDRA-related systems. It is to be emphasized that once k_m is determined for a given test of a sorbate/sorbent system, the other tests of that sytem (at different flowrates and partial pressures) are predictively modeled.

In all tests, there was a subsampler used to measure water dew point or carbon dioxide partial pressure; the volumetric flow rate for the subsamplers was fixed at 0.7 LPM. As a result, the upstream flow was set to the intended flow rate plus 0.7 SLPM, so the flow entering the sorbent bed should be within ~10% of the intended SLPM. Due to using standardized flow meters, the actual volumetric flowrate into the bed is typically ~10% higher than the SLPM values listed for these experiments.

The COMSOL results for the predicted and experimentally measured exit temperatures and vapor pressures are shown in the following figures. In some cases, multiple nominally identical tests were run, while in others only a single test is discussed. Sometimes multiple flowrates and inlet partial pressures were tested, sometimes only one

condition was tested. The derived values of k_m used for the various sorbent/sorbate systems are listed in Table 3. It can be seen that k_m varies by a factor of 5, with 0.002 s^{-1} being a typical value.

Table 3. COMSOL Derived Mass Transfer Coefficients

Sorbent/Sorbate System	k_m s^{-1}
Sylobead/H_2O	0.002
Grade 40/H_2O	0.00125
Grade 544/H_2O	0.0007
RK38/CO_2	0.003
Grade 522/CO_2	0.0035

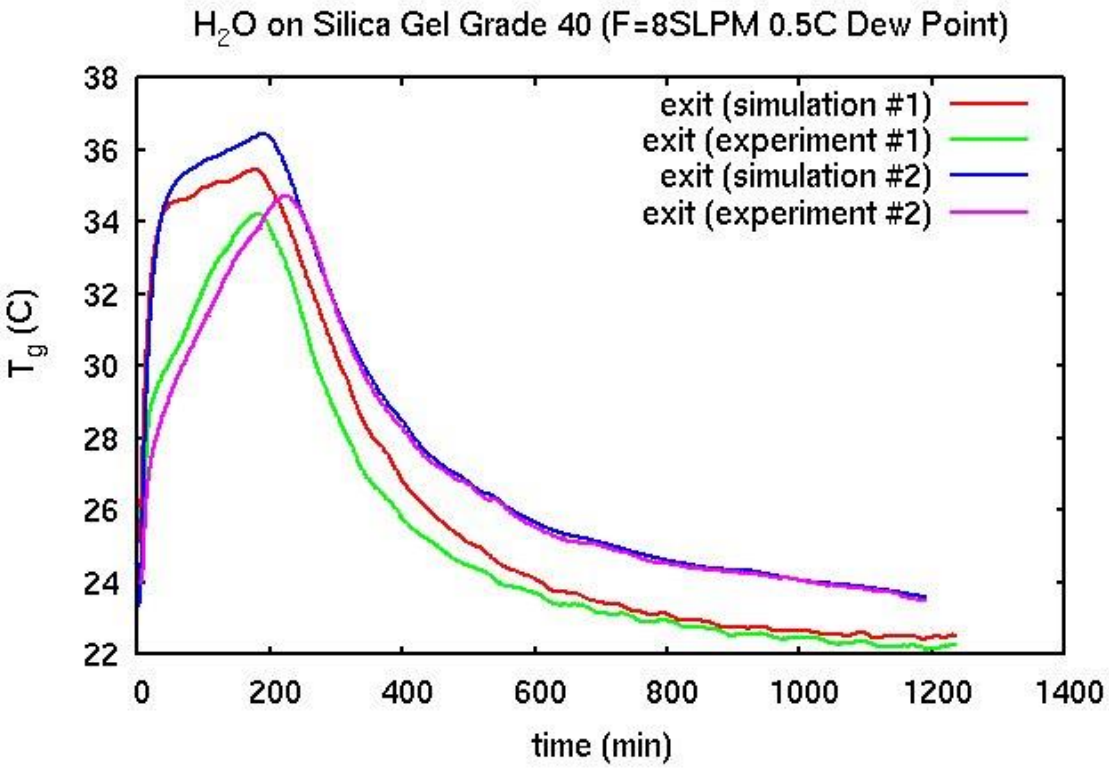

Figure 3. Temperatures for SG Grade 40 8 SLPM 0.5°C Dew Point.

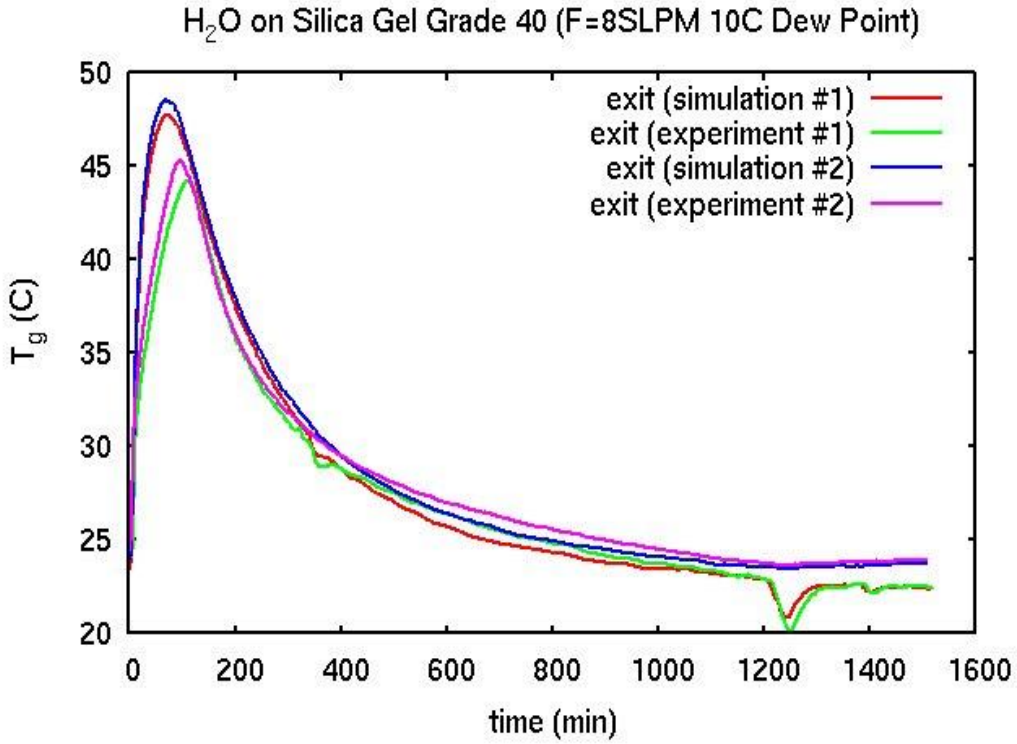

Figure 4. Temperatures for SG Grade 40 8 SLPM 10°C Dew Point.

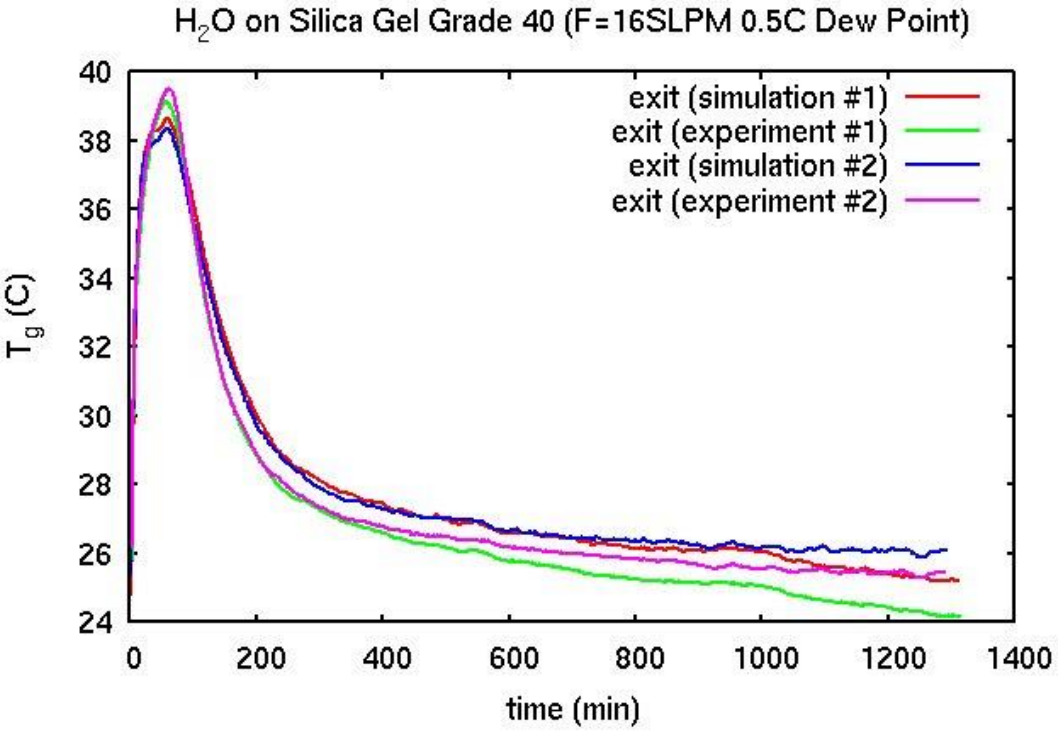

Figure 5. Temperatures for SG Grade 40 16 SLPM 0.5°C Dew Point.

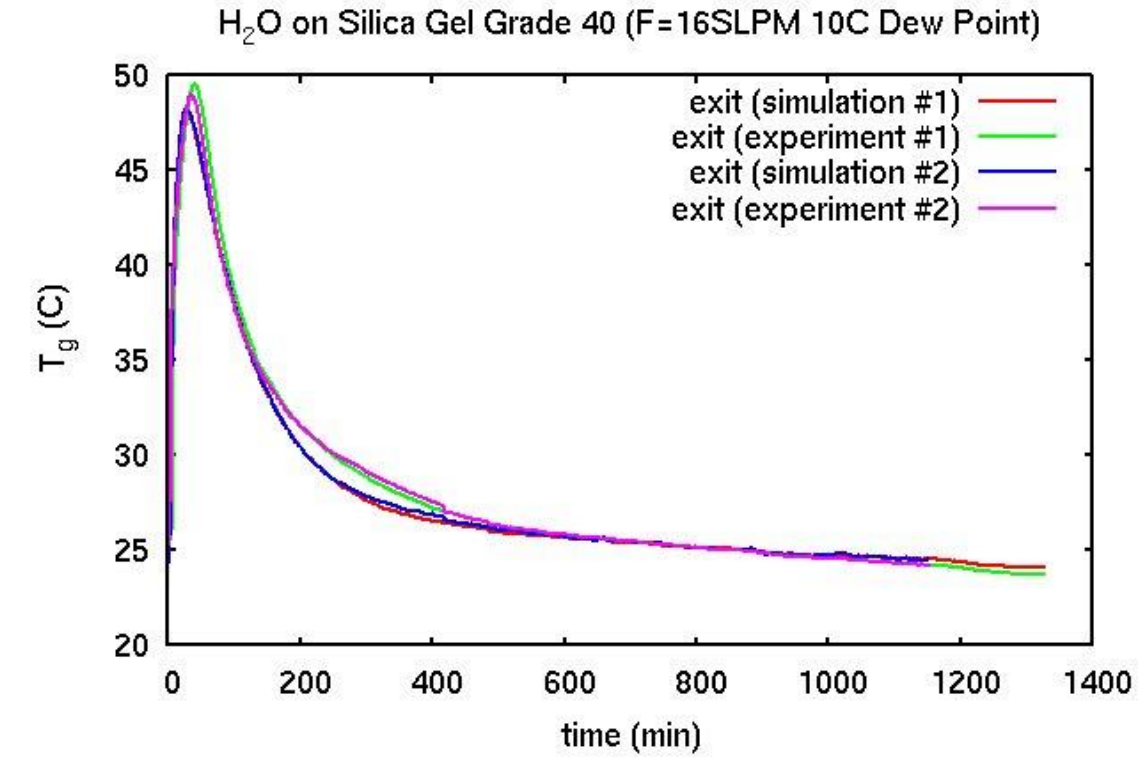

Figure 6. Temperatures for SG Grade 40 16 SLPM 10°C Dew Point.

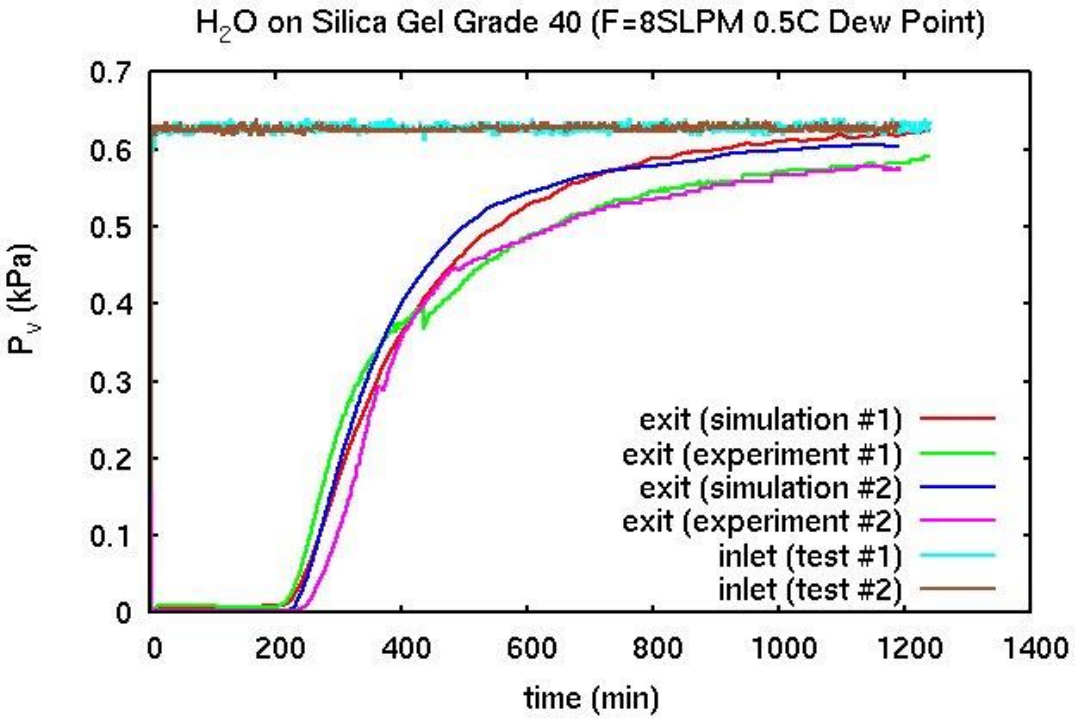

Figure 7. Vapor pressures for SG Grade 40 8 SLPM 0.5°C Dew Point.

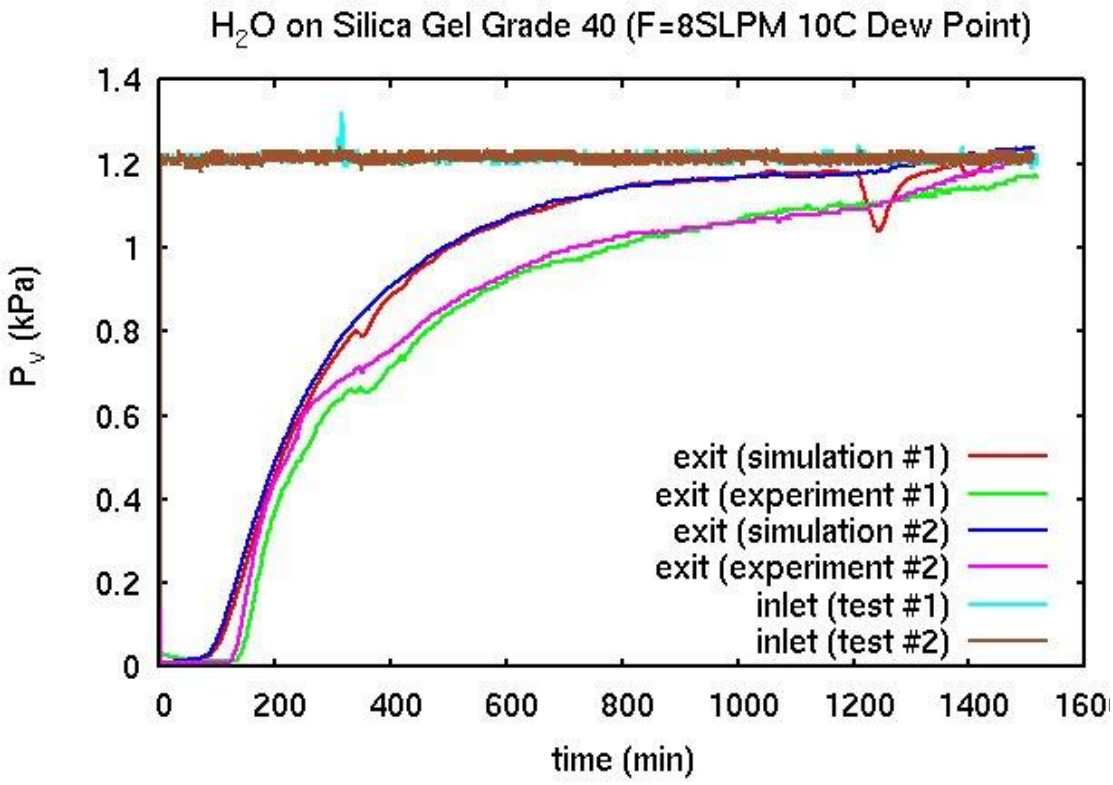

Figure 8. Vapor pressures for SG Grade 40 8 SLPM 10°C Dew Point.

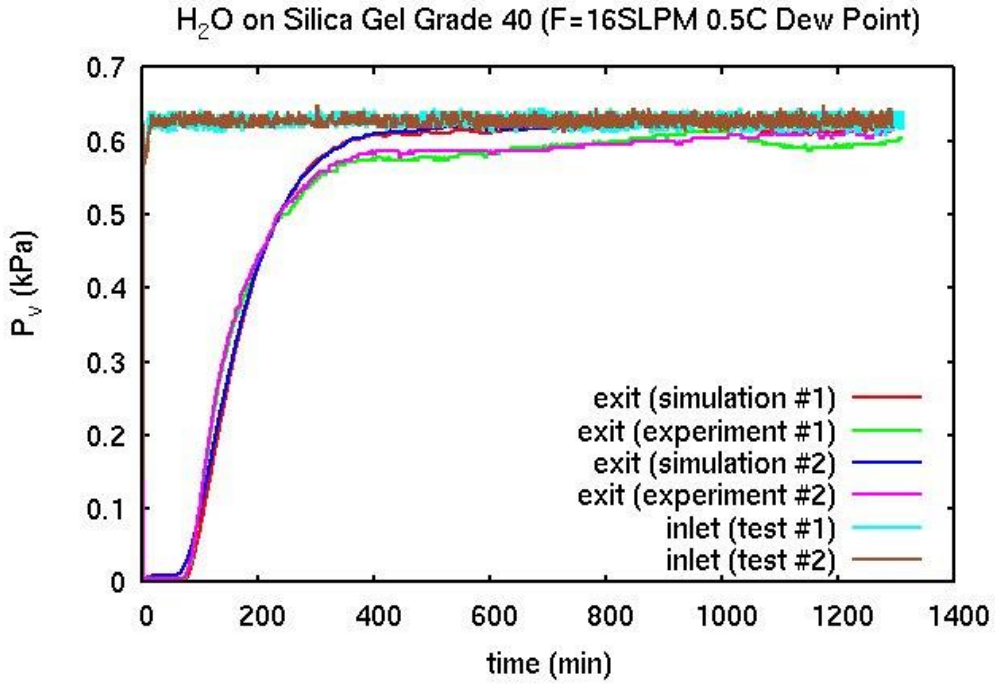

Figure 9. Vapor pressures for SG Grade 40 16 SLPM 0.5°C Dew Point.

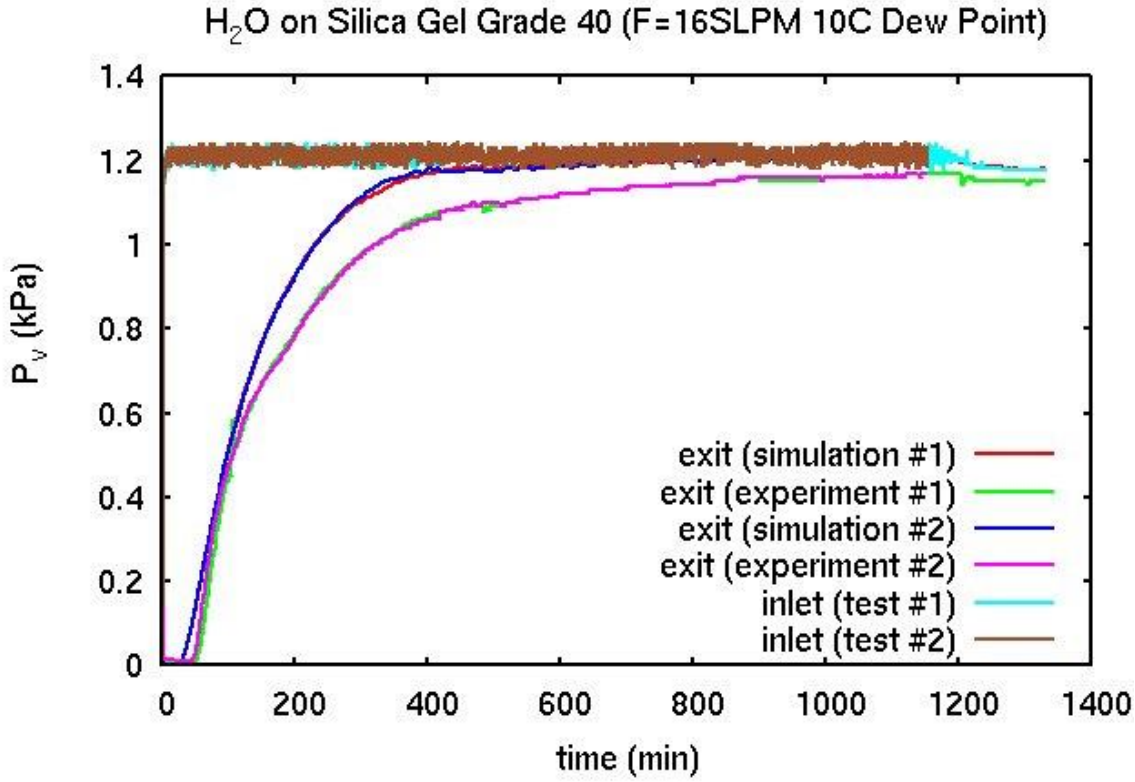

Figure 10. Vapor pressures for SG Grade 40 16 SLPM 10°C Dew Point.

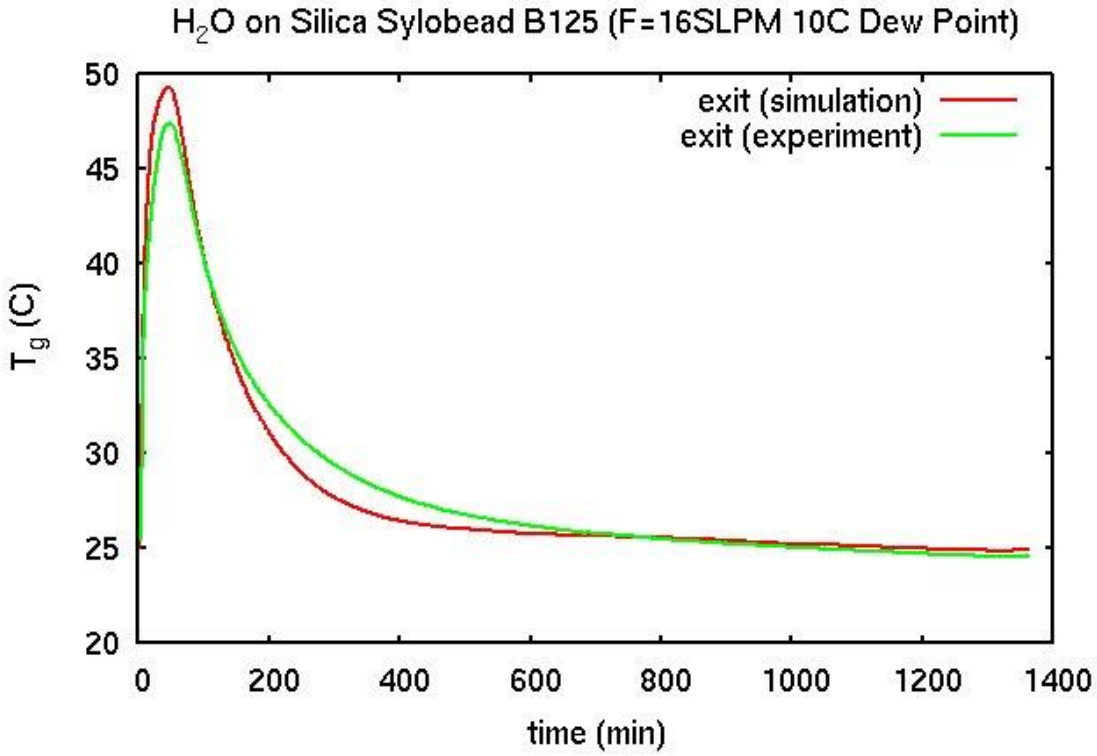

Figure 11. Temperatures for SG Sylobead 16 SLPM 10°C Dew Point.

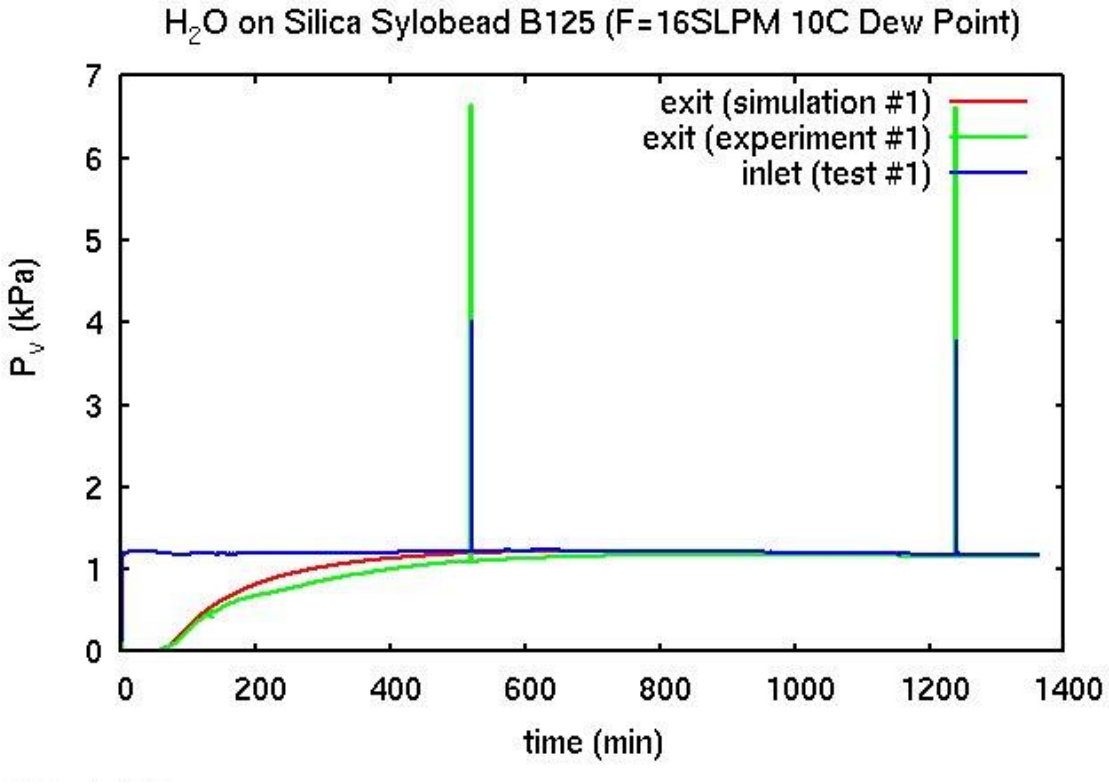

Figure 12. Vapor pressures for SG Sylobead 16 SLPM 10°C Dew Point.

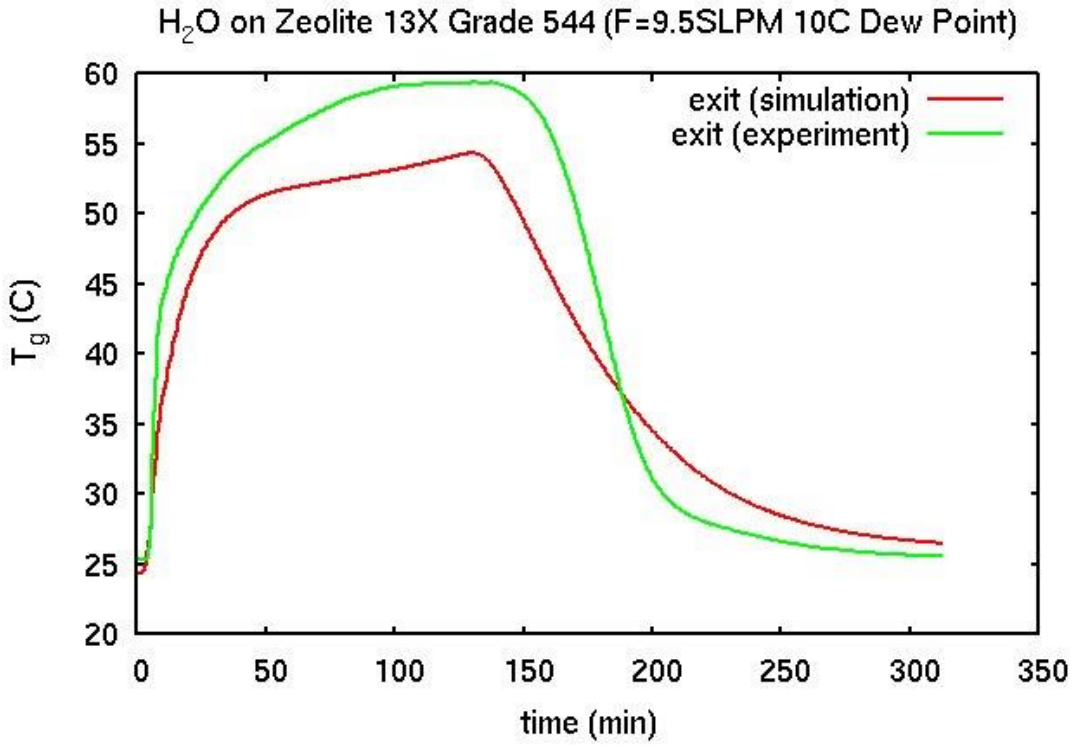

Figure 13. Temperatures for 13X Grade 544 9.5 SLPM 10°C Dew Point.

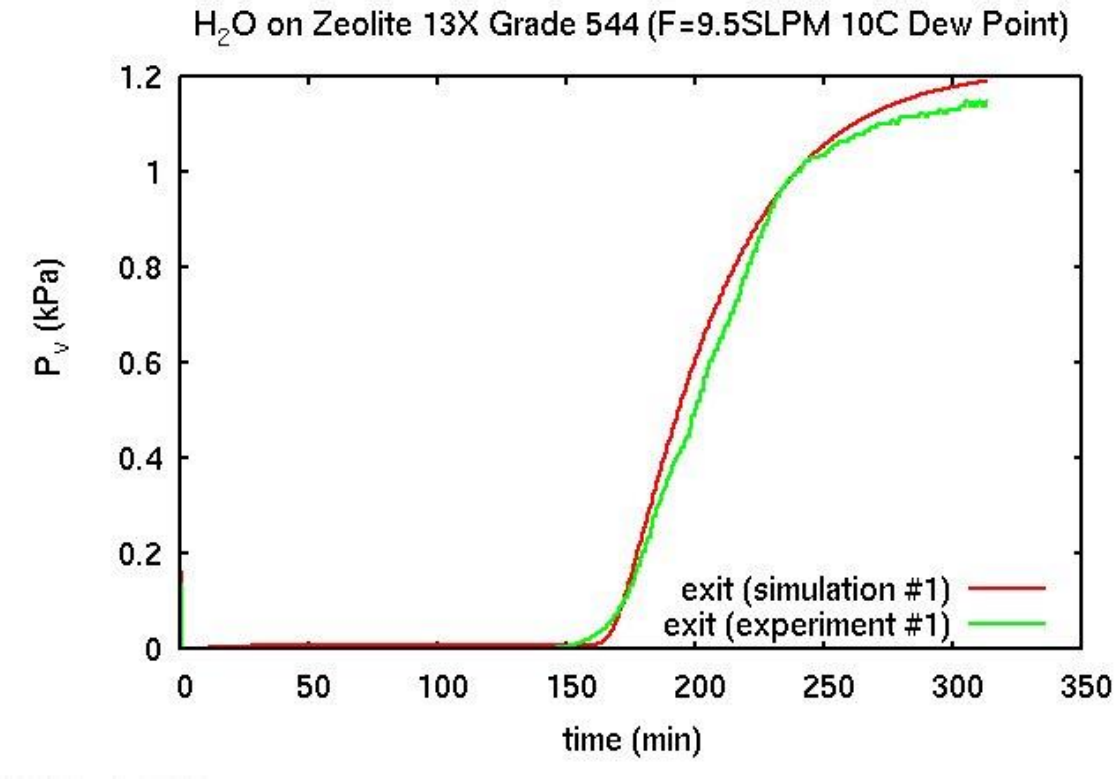

Figure 14. Vapor pressures for 13X Grade 544 9.5 SLPM 10°C Dew Point.

1. *H_2O on Silica Gel Grade 40*

Two flowrates, 16 SLPM and 8 SLPM, and two inlet partial pressures, corresponding to dew points of 0.5°C and 10°C, were run with silica gel Grace Grade 40 sorbent. The two flowrates correspond to Reynolds numbers of ~150 and ~70, respectively. At least 2 tests were run at each condition, though only two tests for each condition are discussed here. Figures 3 to 6 show the temperatures and Figs. 7 to 10 show the vapor pressures. The results show significant variation between and within tests (see, e.g., Fig. 3 and Fig. 7). The most significant temperature difference between the COMSOL models and the experiments appears as a 'hump' at low flowrate and low dew point (Fig. 3). The hump is visible in Fig. 5 as well, but is much smaller in amplitude. The hump is due to too large of an initial rise in temperature (also evident in Fig. 4), followed by a near-leveling off that is not seen in the data, though Fig. 5 only shows the latter. All of this suggests issues with the correlations breaking down at low flowrate and/or vapor pressures. The partial pressure results show that the data at late times do not approach the inlet values; the reason for this consistent deficiency is unknown but may be related to calibration issues with the dew point sensors, since it does not occur in the CO_2 tests (see below). Also, some of the temporal variation in the data are real (reflected in simultaneous changes in temperature and vapor pressure), while some are not; in the models, all are taken as real so that some variations (see, e.g., Fig. 8) are incorrectly propagated (but for the right reasons). The modeled temperature rise 1 inch inside the bed inlet is slower than observed in the experiments (not shown in the figures) due to the flux boundary condition resulting in the inflowing sorbate concentration not immediately rising to the experimental inlet value; this is true in all of the H_2O CBT models to various degrees.

2. *H_2O on Silica Gel Sylobead B125*

Only one flow condition was tested for the Sylobead B125 sorbent: 16 SLPM and 10°C dew point. Figs. 11 and 12 show the model and experiment results for the temperature and water partial pressure, respectively. The comparison is not as good as for Grade 40. This is likely due to two factors. First, the Sylobeads have a significantly different size and shape distribution, such that the packed mean porosity is significantly different (see Table 2) and thus resulting in a different flow field in the bed. Second, the used density, heat capacity, and Toth parameters were derived for Grace Grade 40, not the Sylobead B125 sorbent.

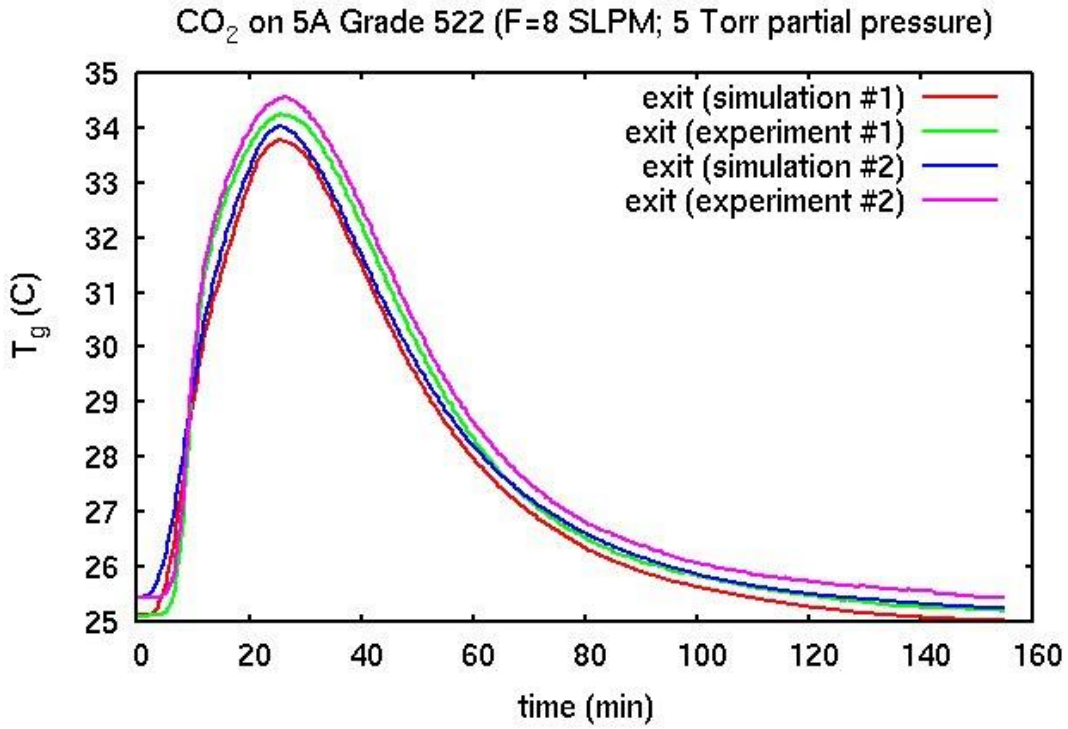

Figure 15. Temperatures for 5A Grade 522 8SLPM 5 Torr partial pressure of CO_2.

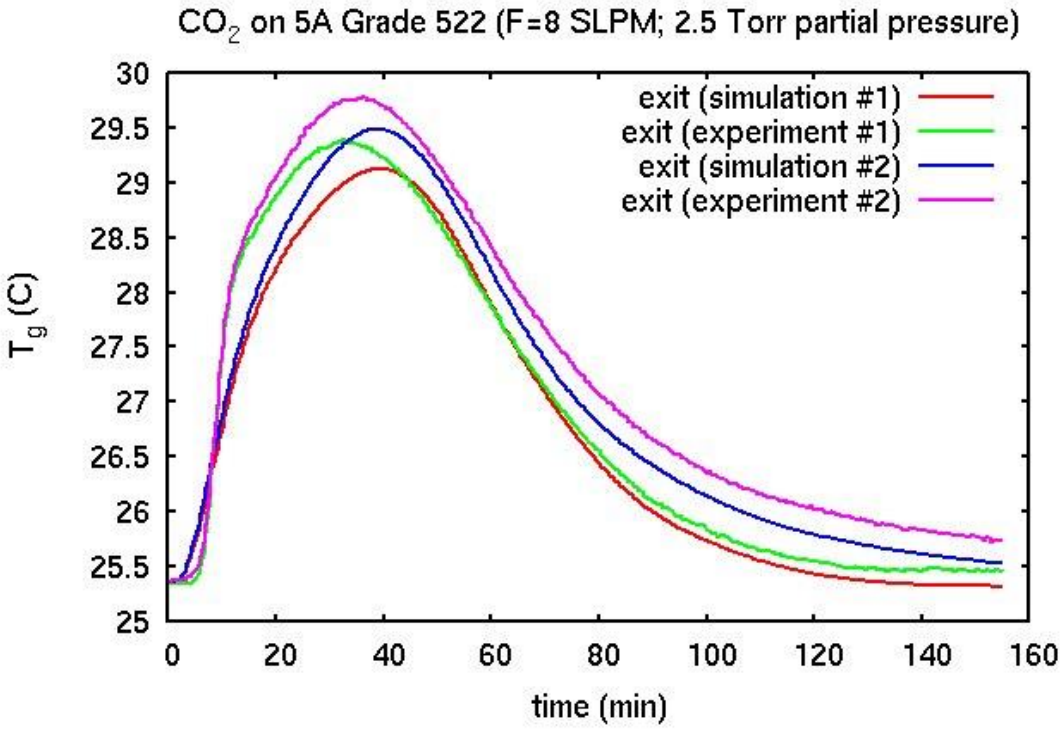

Figure 16. Temperatures for 5A Grade 522 8 SLPM 2.5 Torr partial pressure of CO_2.

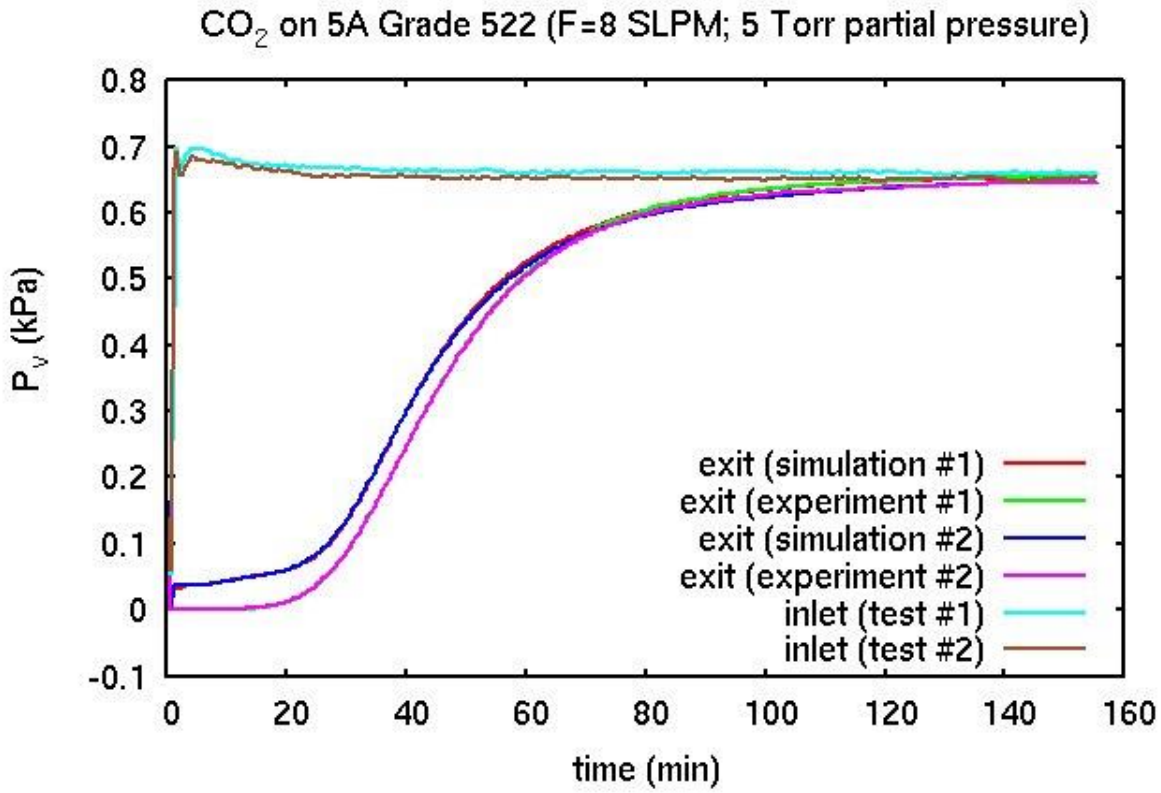

Figure 17. Partial pressures for 5A Grade 522 8 SLPM 5 Torr partial pressure of CO_2.

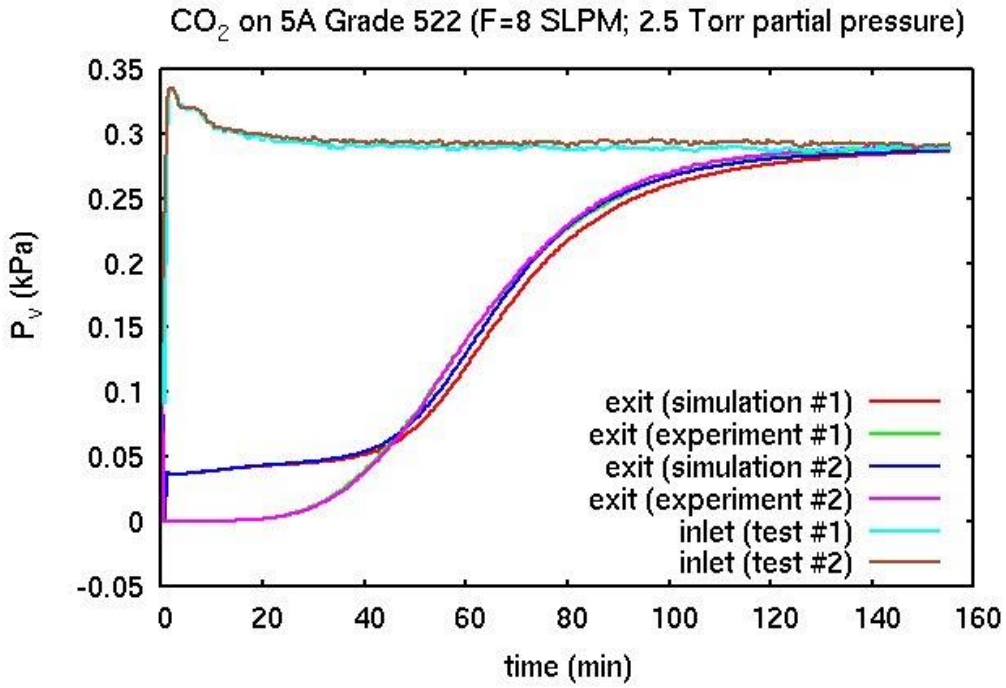

Figure 18. Partial pressures for 5A Grade 522 8 SLPM 2.5 Torr partial pressure of CO_2.

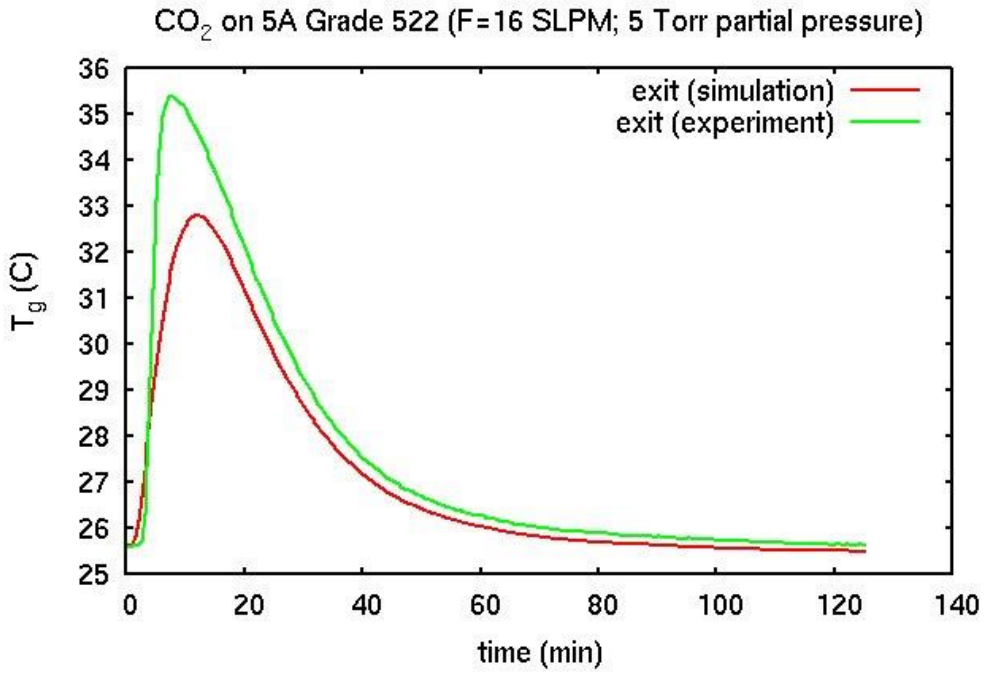

Figure 19. Temperatures for 5A Grade 522 16 SLPM 5 Torr partial pressure of CO_2.

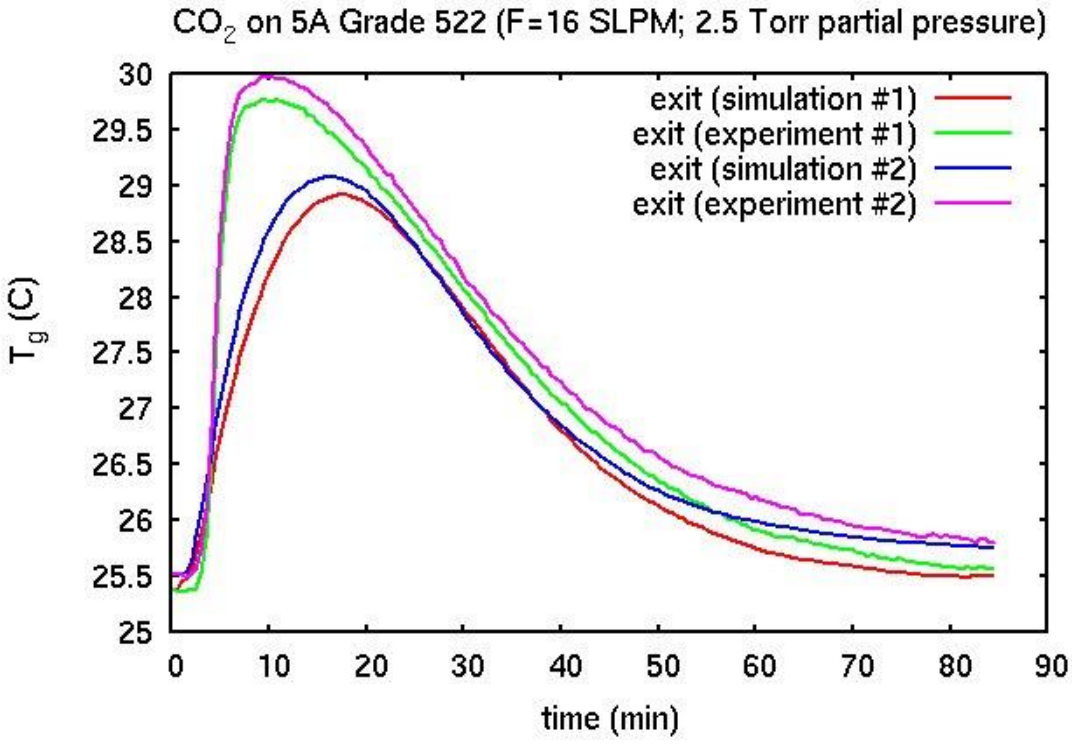

Figure 20. Temperatures for 5A Grade 522 16 SLPM 2.5 Torr partial pressure of CO_2.

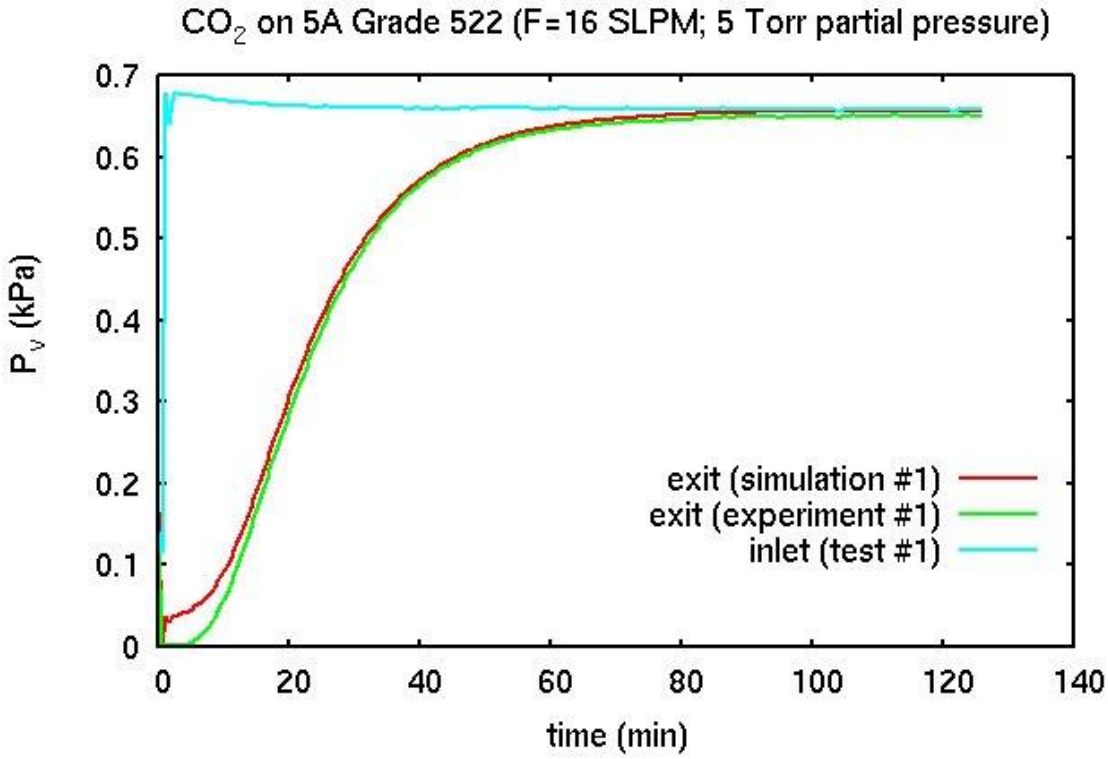

Figure 21. Partial pressures for 5A Grade 522 16 SLPM 5 Torr partial pressure of CO_2.

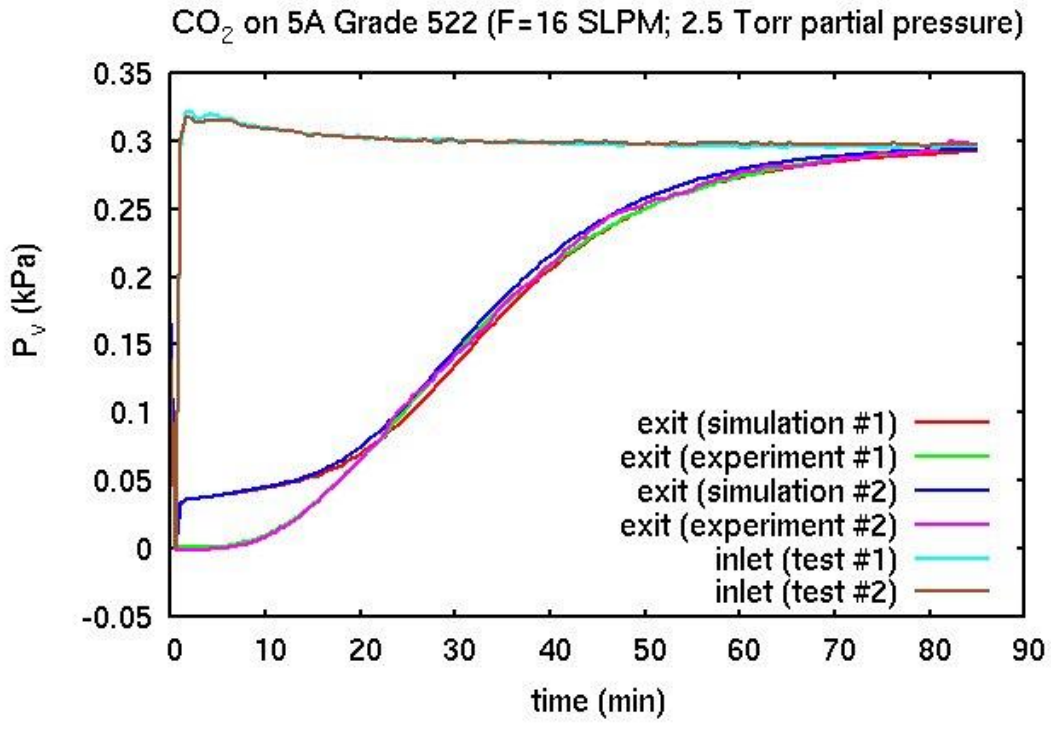

Figure 22. Partial pressures for 5A Grade 522 16 SLPM 2.5 Torr partial pressure of CO_2.

3. *H_2O on 13X Zeolite Grade 544*

Only one CBT experiment was conducted with H_2O on Grace Grade 544 due to difficulties in regenerating the bed. The inlet pressure, pressure drop, and ambient conditions were not recorded; they are assumed to be comparable to the other tests. The inlet water vapor partial pressure was 1.2 kPa, corresponding to a dew point of 10°C. Although the flowrate was supposed to be 16 SLPM, the flow meter reference settings and calibrations may have been off for this test. Thus, the results given here in Figs. 13 and 14 assume an actual flowrate of 9.5 SLPM. This gives a good fit to the water vapor rise curve (Fig. 14). The temperature peak in the model is too low and drops off too slowly compared to the data. A combination of higher heat of adsorption and poor insulation would be required to explain this. However, another explanation, instead of a low flowrate, is that the porosity was substantially incorrect, due to, for example, in incorrect bulk pellet density or gross non-sphericities in the pellets, as well as the pellets starting with an initially extremely low loading (as if coming straight from bake out with no N_2 flow to equilibrate the temperature in the bed).

4. *CO_2 on 5A Zeolite Grace Grade 522*

It is well known that CO_2 competes with H_2O on zeolites for adsorption, with water being much more easily adsorbed. Thus, for the CO_2 CBT experiments, since the purge gas is not perfectly dry (the purge has a dew point of ~-70°F), a larger initial loading is assumed in order to mimic the H_2O loading that would occur during the N_2 purge. For Grade 522, an initial uniform loading of 350 mol/m^3 was thus assumed. This is an approximation based on the equilibrium water loading of Grade 522, but, as a result, the model does not properly capture the initial partial pressure breakthrough curve. Two flowrates, 16 and 8 SLPM, and two inlet partial pressures, 2.5 and 5.0 Torr, were run for CO_2 on 5A Grade 522 sorbent. Multiple tests were run at each condition except for 16 SLPM and 5 Torr. Comparisons between the experiments and the COMSOL models are shown in Figs. 15 through 22. As expected, the model consistently misses the gentle initial rise of the 'heel' of the CO_2 partial pressure curves, particularly at low partial pressures. In addition to the artificial initial loading, this is also likely due to the 1-D model not being able to capture the channel flow near the walls, where breakthrough will occur more quickly; CO_2 adsorption is more sensitive to this effect than H_2O since it occurs more than ~5x more quickly (compare, for example, Figs. 4 and 15). A better approach may be to turn off loading in some initial depth of the bed where water prevents any CO_2 loading; this is left for future work since the precise details of the purge (duration, sorbate partial pressure, volumetric flowrate) are not known for the purge gas used in the CBT experiments. In addition, the model peak temperatures, particularly for the high flow rate tests, are consistently too low. This may be due to an inaccurate heat of adsorption or the fact that the *Nu* correlations used to estimate thermal coefficients were based primarily on H_2O data, not CO_2 data. For the CO_2 tests on both Grade 522 and RK38 (see below), the sorbent pellets were sieved with an 8x12 sieve, reducing the spread of particle size in the bed to between 2.38 and 1.41mm. Other tests using a 20x50 sieve (not discussed here further) for Grade 522 showed very similar results.

5. *CO_2 on 5A Zeolite RK38*

The initial loading for the CO_2 on RK38 tests was set to 250 mol/m^3. Two flowrates, 16 and 8 SLPM, and two inlet partial pressures, 2.5 and 5.0 Torr, were run. Multiple tests were run at each condition except for 16 SLPM and 2.5 Torr. Comparisons between the experiments and the COMSOL models are shown in Figs. 23 through 30. Again, as expected, the model consistently misses the rise of the CO_2 partial pressure curves. In addition, due to the initial non-equilibrium loading, there are some numerical instabilities in the sorbate concentration at initial times which show up as wiggles in the 5 Torr partial pressure plots (see, e.g., Fig. 25). Also, as for Grade 522, the model peak temperatures are too low, particularly at high flow rates. This suggests that issues with the CO_2 model or testing procedure in general are more likely the problem than sorbent-specific properties such as the heat of adsorption.

The adsorption capacity, the moles of sorbate per unit mass of sorbent that the system can adsorb, was measured for the 16 SLPM 5 Torr flow condition tests to be 1.15±0.05 mol/kg. In the models, the loading throughout the bed is within a few percent of the equilibrium loading by the end of the tests. Thus, the calculated theoretical capacity is q_*/ρ_s; it falls within the uncertainty range of the measured values. This argues against any significant fraction of the sorbent in the bed being 'inactive' due to the presence of water. Another possibility is that all of the CO_2 Toth isotherms for zeolites[11] were derived with sorbents that were contaminated with some unknown amount of H_2O due to too low of an activation temperature. This would make them inaccurate at low CO_2 loading levels.

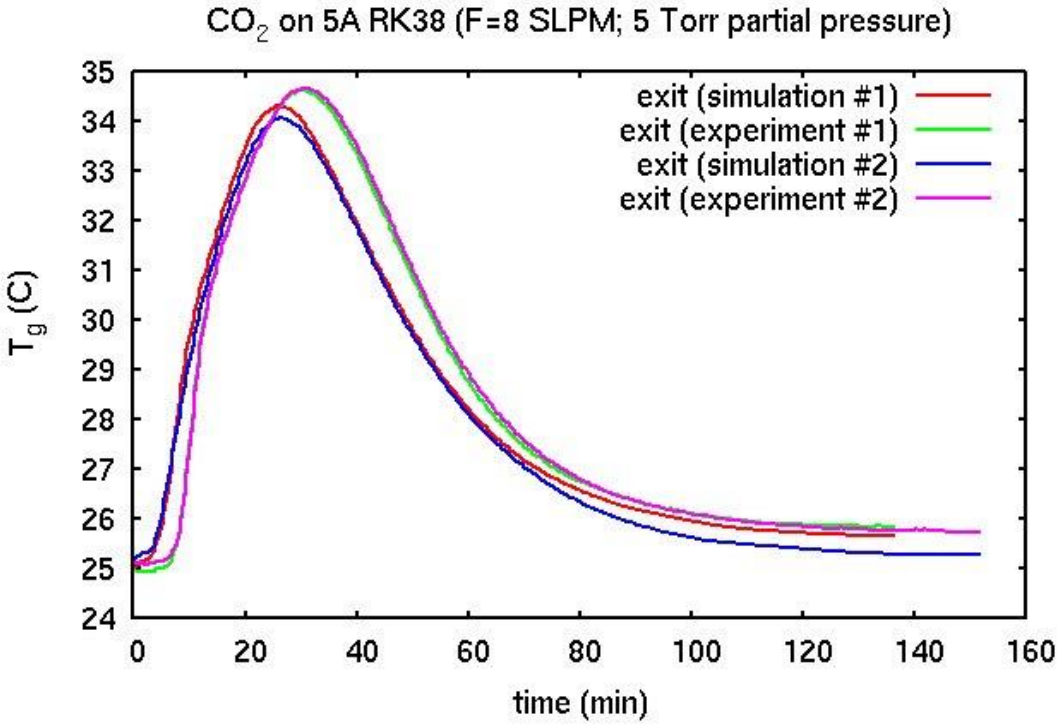

Figure 23. Temperatures for 5A RK38 8 SLPM 5 Torr partial pressure of CO_2.

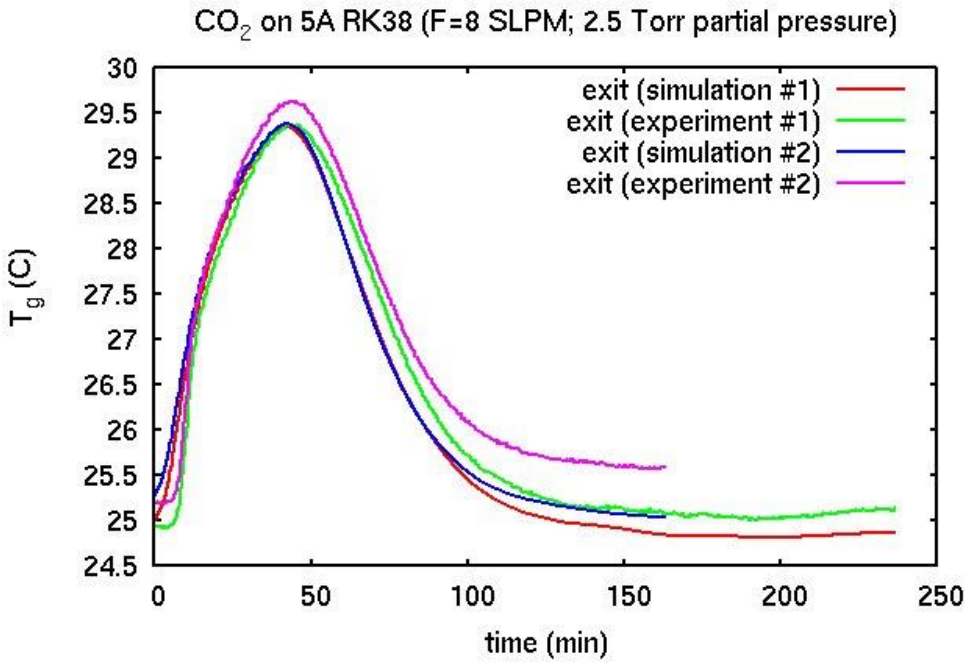

Figure 24. Temperatures for 5A RK38 8 SLPM 2.5 Torr partial pressure of CO_2.

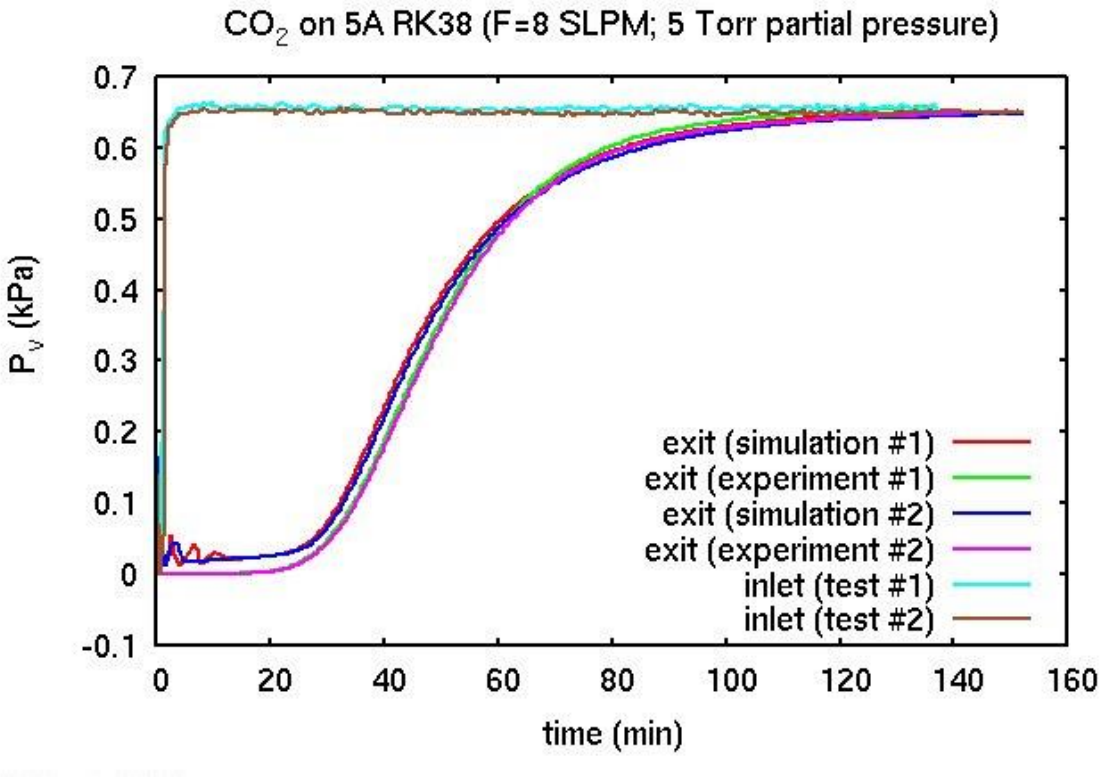

Figure 25. Partial pressures for 5A RK38 8 SLPM 5 Torr partial pressure of CO_2.

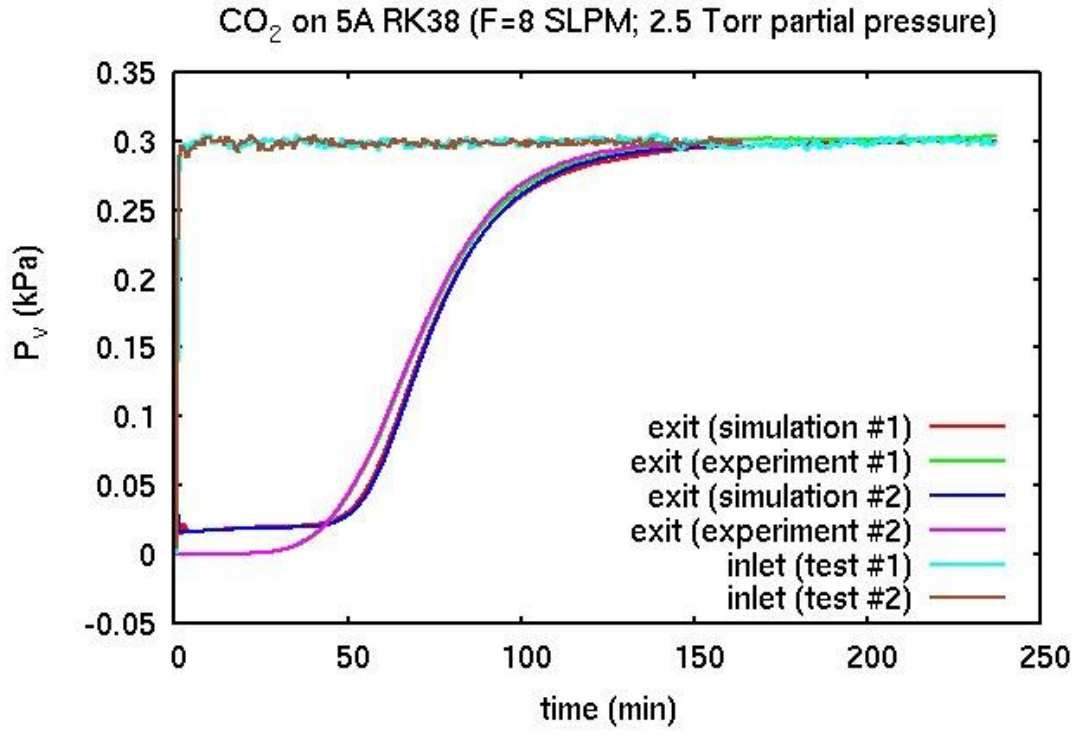

Figure 26. Partial pressures for 5A RK38 8 SLPM 2.5 Torr partial pressure of CO_2.

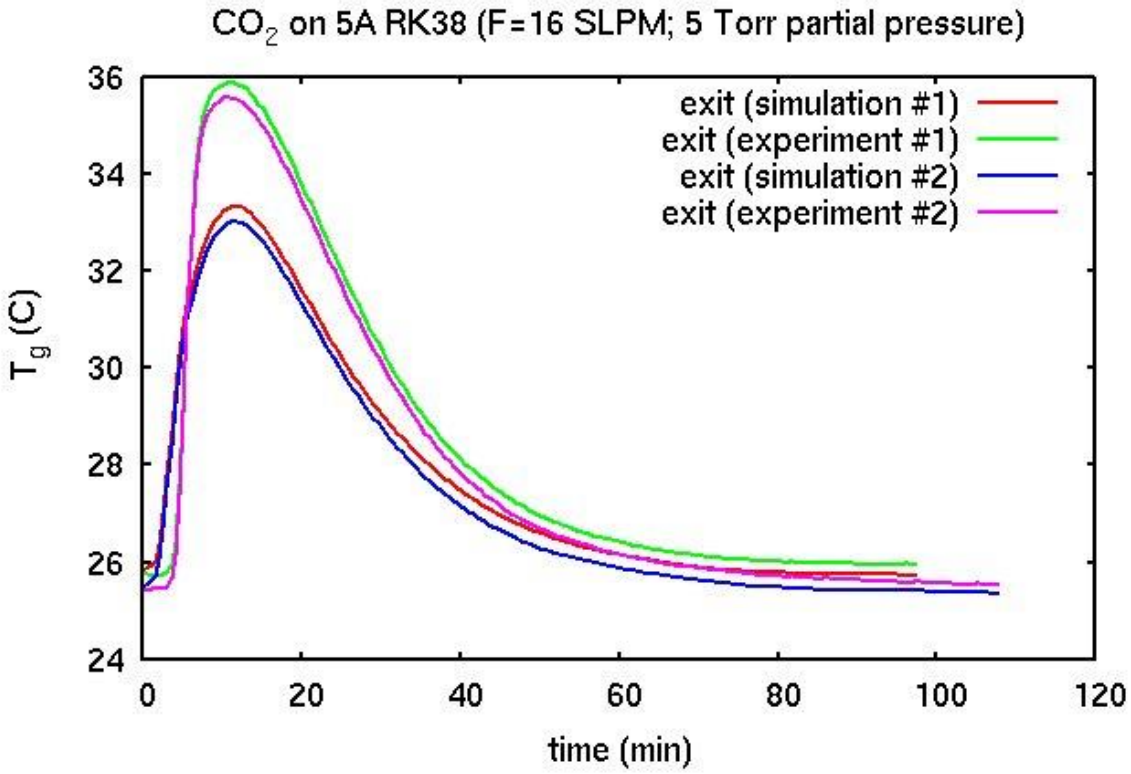

Figure 27. Temperatures for 5A RK38 16 SLPM 5 Torr partial pressure of CO_2.

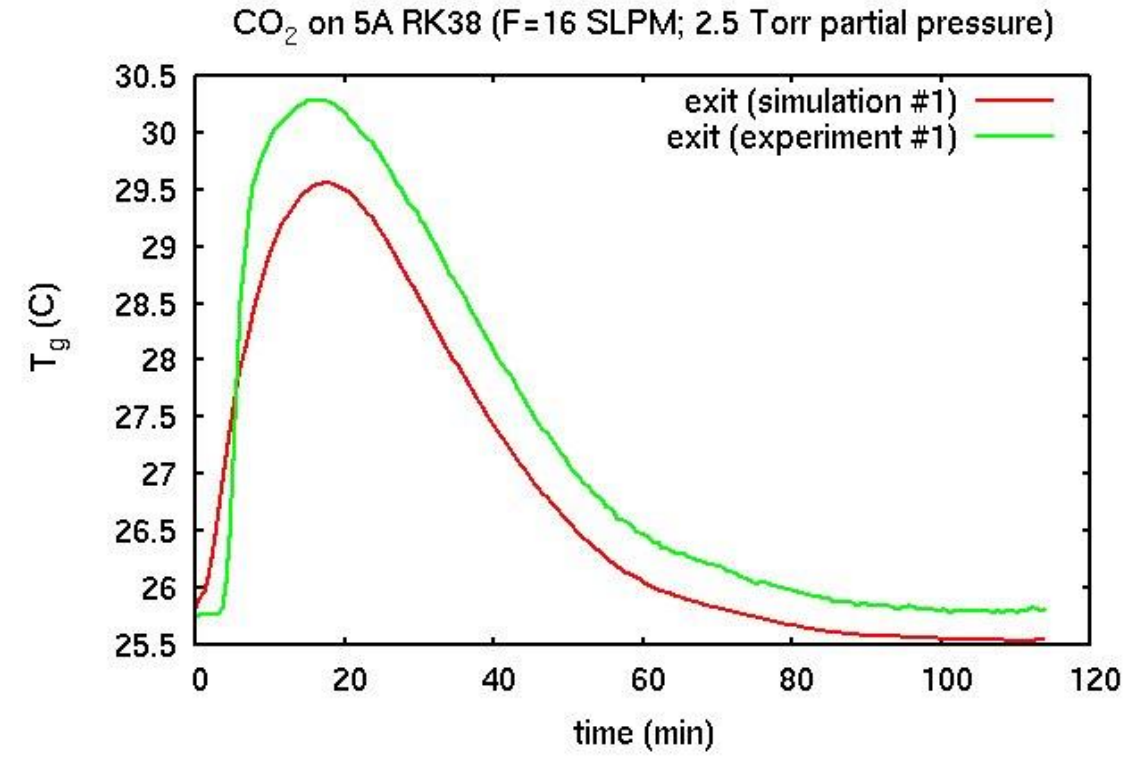

Figure 28. Temperatures for 5A RK38 16 SLPM 5 Torr partial pressure of CO_2.

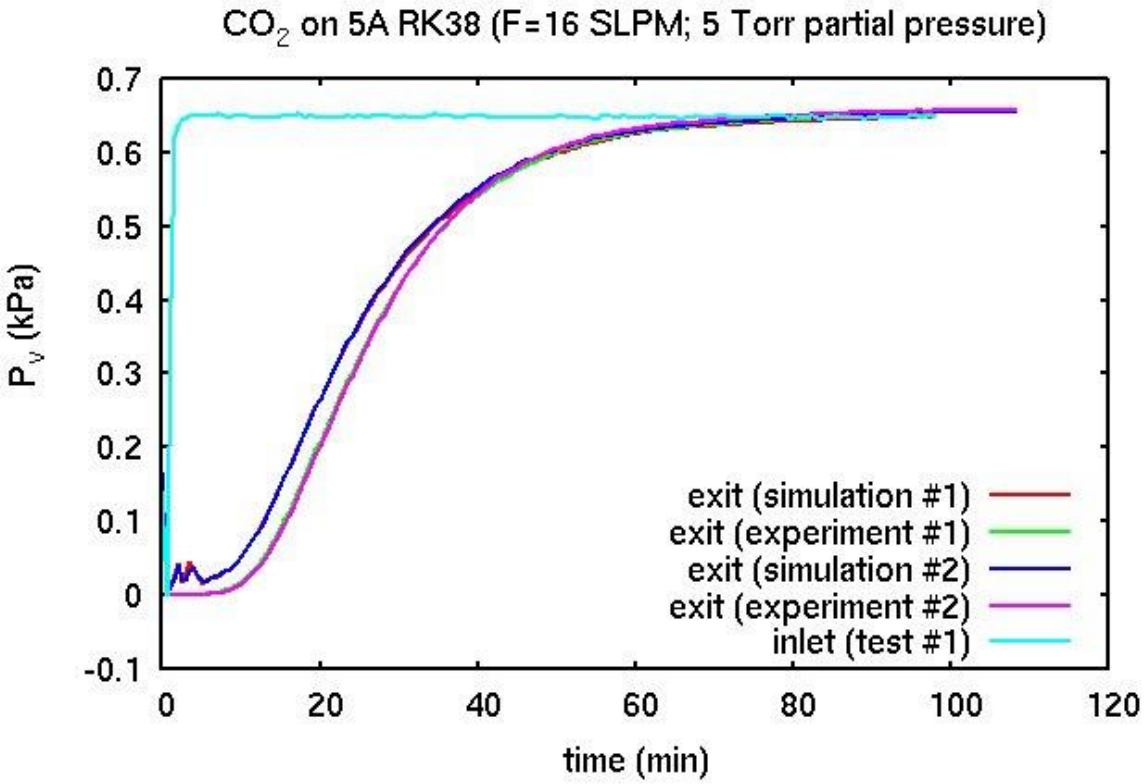

Figure 29. Partial pressures for 5A RK38 16 SLPM 5 Torr partial pressure of CO_2.

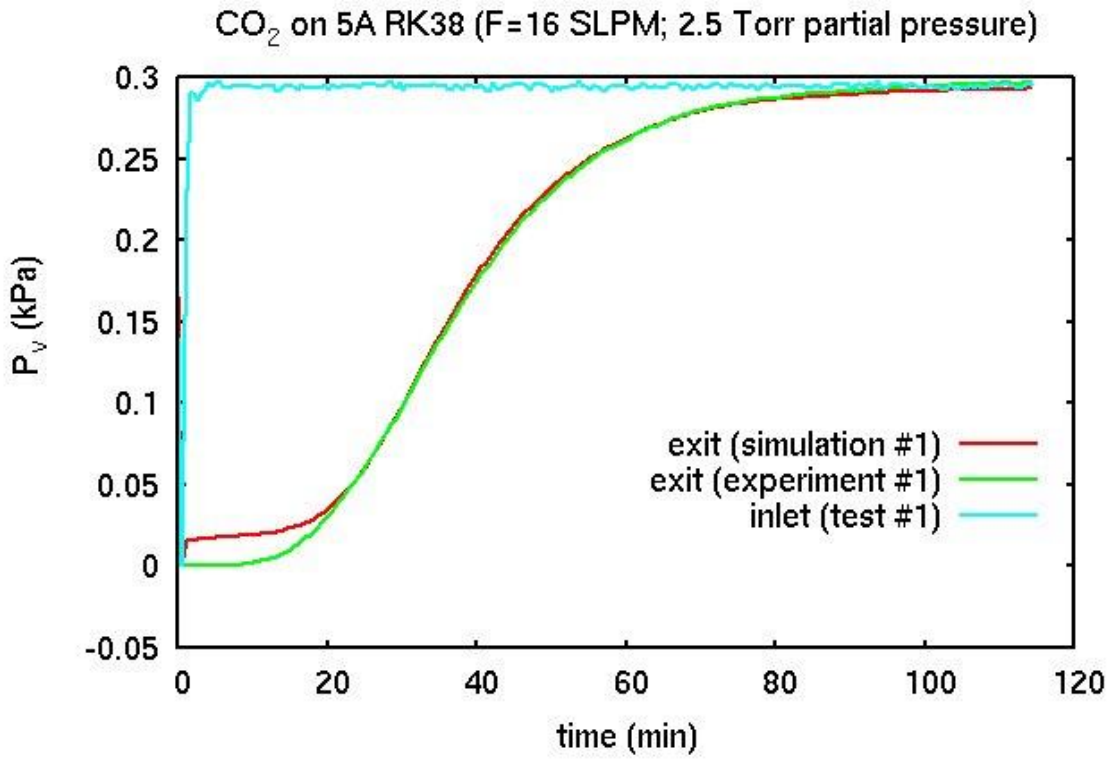

Figure 30. Partial pressures for 5A RK38 16 SLPM 2.5 Torr partial pressure of CO_2.

IV. Conclusion

Using COMSOL, we have been able to derive a predictive model for adsorption physics in a variety of flowrate and sorbate partial pressure regimes and for a variety of sorbents. For water vapor on silica gel and zeolites, the limitations are in general due to the experimental data, not the model, due to variations and uncertainties in the dew point measurements, the ambient conditions, and unsteady flow conditions. For carbon dioxide on zeolites, the model does not compare as well to the data. However, it is not clear if this is a deficiency of the model, such as the LDF, which uses a single constant parameter to determine the loading rate, or of the experiments, due to competing pellet loading from water vapor in the purge gas. Future CO_2 tests will need to carefully track the amount of H_2O loading on the sorbent for any given test. In addition, the 1-D nature of the model is not capturing some of the physics due to channeling of the carrier gas near the walls of the sorbent bed. Future work will extend the PDEs used here to 2-D axisymmetry and will include the impact of using a radially dependent porosity due to packing. Since no purge gas is perfectly dry, another extension of this work is to include binary Toth relationships, particularly for the CO_2, in order to properly capture the competition between H_2O and CO_2. Also, it is known[13] that the heat of adsorption decreases with increasing loading; this effect, when known, will be incorporated in future models. The values of k_m found in this work will be used in broad applications of sorbent/sorbate systems to estimate performance without the need of testing.

References

[1]Perry, J. L., et, al., "Integrated Atmosphere Resource Recovery and Environmental Monitoring Technology Demonstration for Deep Space Exploration," *International Conference on Environmental Systems*. AIAA, San Diego, 2012.

[2]Knox, J.C., et. al., "Development of Carbon Dioxide Removal Systems for Advanced Exploration Systems," *International Conference on Environmental Systems*. AIAA, San Diego, 2012.

[3]COMSOL, COMSOL Multiphysics®, 2009.

[4]Rumpf, H., and Gupte, A.R., "The influence of porosity and grain size distribution on the permeability equation of porous flow", Chemie Ing. Techn. (Weinheim), v. 43, no. 6, p 367-375, 1975.

[5]Ergun, S., Chem. Eng. Prog., 48, 89, 1952.

[6]D. M. Ruthven, Principles of Adsorption and Adsorption Processes, Wiley Interscience: New York, 1984.

[7]M.F. Edwards and J.F. Richardson, Chem. Eng. Sci. 24, 607 (1969).

[8]Wakao, N. and Kaguei, S.1982 Heat And Mass Transfer In Packed Beds, Gordon and Breach, New York.

[9]Li, C.H., and Finlayson, B.A. 1977 Heat transfer in packed beds - a reevaluation Chem. Eng. Sci.32 1055-1066.

[10]E.L. Cussler, Diffusion: Mass Transfer in Fluid Systems, 2nd Edition (Cambridge University. Press, London, 1997.

[11]Wang, Y. and Levan, M.D. "Adsorption Equilibrium of Carbon Dioxide and Water Vapor on Zeolites 5A and 13X and Silica Gel: Pure Components", Journal of Chemical and Engineering Data, 54(10), 2839-2844, 2009.

[12]Ritter, J.A., and Ebner, A.D., "Design of an Adsorption-Based Carbon Dioxide, Humidity and Trace Contaminant Removal System", Final Report for Cooperative Agreement NNM05AA10A, 2008.

[13]"Davison Molecular Sieves Adsorption Equilibria", Davison Chemical Report.

[14]Yagi, S. and Kunii, D., "Studies on Heat Transfer Near Wall Surfaces in Packed Beds", AIChE J. 6 543-546, 1960.

[15]Kay, R., and Pancho, D., "Evaluation of Alternative Desiccants and Adsorbents for the Desiccant/Adsorbent Bed", Honeywell Report 12-77742, CAGE 70210, 2013.

[16]Finn, J.E., Ho, E.C., and Knox, J.C., "Progress Report on the 4BMS Adsorption Characterization Study", NASA Ames Research Center, 1995.